Modal sensitivity analysis and TCSC effectiveness

by

Qinghua Liu

A thesis submitted to the graduate faculty

in partial fulfillment of the requirements for the degree of

MASTER OF SCIENCE

Major: Electrical Engineering

Major Professor: Dr. James D. McCalley

Iowa State University

Ames, Iowa

1997

Graduate College
Iowa State University

This is to certify that the Master's thesis of

Qinghua Liu

has met the thesis requirements of Iowa State University

To my parents

TABLE OF CONTENTS

LIST OF TABLES

LIST OF FIGURES

ACKNOWLEDGMENTS

In the first place I wish to express my deep appreciation to Dr. James McCalley for his guidance and encouragement during the course of this work. For many things which I have learned from him, I shall ever be grateful.

Accomplishing this thesis has been a most rewarding experience and much of the credit for that goes to Dr. Yixin Ni and the members of my committee: Dr. James McCalley, Dr. Vijay Vittal and Dr. Scott Hansen. In this respect, I am very grateful to Dr. Yixin Ni for inspiring and fruitful discussions, invaluable suggestions and help.

The power group in I.S.U. has been an exciting and friendly working environment. To my friends in the group, thank you.

I have no words to express what my family has meant to me all these years. To my father and mother, Zenghuang Liu and Yousheng Ma, my brother Yanjia Liu, from the bottom of my heart, thank you.

I sincerely wish that my work and the fine education I have received at I.S.U. will prove beneficial to society and particularly to my country.

ABSTRACT

Thyristor-Controlled Series Capacitors (TCSC) may be applied in transmission systems to improve system dynamic performance. One of the important aspects of designing a TCSC controller to provide additional damping is to identify the most effective TCSC location for the required control objective because for a meshed power system, the effectiveness of TCSC control varies with the TCSC installation location. Two methods are presented to determine the potential TCSC location to control a certain swing mode. The basis of these methods are modal sensitivity analysis. A multi-machine eigenvalue sensitivity program is developed, which enables us to calculate eigenvalue sensitivity with respect to line susceptance (parameter sensitivity) and eigenvalue sensitivity with respect to transfer function of TCSC (functional sensitivity), and thus determine the most effective TCSC location.

1 INTRODUCTION

1.1 The need for FACTS controllers in AC systems

1.1.1 What is FACTS?

Research institutions, utilities, and manufacturers throughout the world are pursuing programs with two main objectives [1]:

- to increase the power transfer capability of transmission networks
- to provide direct control of power flow over designated transmission routes

While economics remain an important aspect, the current environment of deregulation and constraints on building more transmission facilities provides compelling reasons to develop alternative approaches. Mature power electronic based equipment can be considered a dependable means to help achieve these goals. It is this aspect which is the focus of *flexible AC transmission systems* (FACTS) controller development.

FACTS has been defined by the IEEE as "alternating current transmission systems incorporating power electronic-based and other static controllers to enhance controllability and increase power transfer capability" [2]. The collective acronym FACTS has been adopted in recent years to describe a wide range of controllers, many of them incorporating large power electronic converters, which may, at present or in the future, be used to increase the flexibility of power systems and thus make them more controllable. Some of these controllers are already well established and some are still in the research

or development stage. HVDC and SVC are examples of power electronic systems which are already well established. Thyristor controlled series capacitors (TCSC) and unified power flow controller (UPFC) are examples of power electronic systems which are still in the development stage [3].

1.1.2 Influence of restructured power industry

In the past, North American transmission systems, owned by regulated, vertically integrated utility companies, have been designed and operated so that conditions in close proximity to security boundaries were not frequently encountered. One reason for this was that the load patterns and consequently the power flow directions were fairly predictable and they were not significantly different from that for which they were originally designed. Another reason was that companies could usually justify construction of new facilities if they could show reliability would be compromised otherwise.

During 1993, the electric power industry in the United States started a period of unprecedented change as a result of the Energy Policy Act of 1992. Among other provisions, this act mandates wholesale access to utility transmission systems by non-utility-and largely unregulated-generators. Given the different regulatory oversight and competitive forces for the various parts of the utility business, that act is in effect causing utilities to unbundle their traditional services of generating, transmitting, and distributing power [4].

Generally, vertically integrated utilities are moving toward a more loosely connected, three-part business structure. The generation side of the business is emphasizing least-cost production and wholesale marketing of electric power as a commodity. The transmission side is emphasizing integration and wheeling under set, or yet-to-be-defined, rules, and the distribution side is emphasizing value-added services to meet specific customer needs [4].

In the United States, about 40 percent of the electricity generated is sold by the producing utilities through wholesale transactions to other utilities [4]. Unbundling traditional utility services will probably increase the number of bulk sales and alter the power-flow requirements considerably. Also, more players, including unregulated, independent power producers, some large and some small, and many without high-speed controls, will be using the transmission network to make increasingly complex transactions [4].

Because of normal load growth coupled with the economics of long distance energy exchange, transmission usage continues to increase. Also competition, coupled with regulatory and environmental requirements, has caused construction of new transmission facilities to be significantly inhibited. As a consequence, the transmission systems are being required to accommodate flow patterns for which they were not originally designed.

When trying to improve transmission system use, a key assumption is that the existing system reliability will be maintained. This assumption has two major aspects: adequacy and security. Adequacy may be defined as the ability of the power system to meet energy demands, within component ratings and voltage limits [5]. Security may be defined as the ability of the power system to withstand incidents (faults or equipment outages) without uncontrolled loss of customer load [5]. The highly interconnected transmission grids are essentially the glue holding the generators and loads together. From a technical point of view, the greatest challenge posed by open access and increasing competition is to ensure that this "glue" continues to hold, and that the economies of integration enhance interconnected systems without sacrificing system security, even as utilities themselves change fundamentally [4]. At issue is the value of the effort and expense to fully utilize existing transmission systems (more adequacy), without endangering system security. Thus, there is a need for transmission-based controllers to maximize power transfer and maintain system stability. The need exists for two reasons:

- It offers control for thermal, voltage, and transient problem, and can be viewed as having a very low cost/benefit ratio.

- Its system-oriented control function, together with its capability to perform this function located on transmission equipment (instead of generator equipment) is well-suited for the new power industry organizational structure where the only entity having primary responsibility for system problems would be the one that owns the transmission equipment.

An examination of the equation below provides some insight into possible techniques for controlling power flow. This equation, under simplifying assumptions, expresses the power flow across a transmission line terminated at buses 1 and 2.

$$P_{12} = \frac{V_1 V_2}{X} \sin \delta_{12} \tag{1.1}$$

Since voltage magnitudes are tightly constrained to be close to 1.0, whereas X may vary over a much wider range, the impact of changing terminal voltage is small when compared to the impact made by changing the inductive reactance or the relative phase-angle between the two terminals. Thus, altering the natural inductive reactance of a transmission line or transmission corridor will influence the power flow. Similarly, adjusting the relative phase angle, δ_{12}, can determine the magnitude and direction of the power flow.

1.1.3 Power transfer limitations

Technically, limitations on power transfer can always be relieved by the addition of major new transmission and/or generation facilities. The focus of this discussion is on means to achieve the goals without such system changes [1].

Power flow over a transmission system is limited by one or more of the following aspects [3]:

- Stability limits
- Voltage limits
- Thermal overload limits

Each of these limitations includes consideration of significant contingencies, which often are more constraining than normal operation.

1.1.3.1 Stability limits

Generally, the power-transfer constraints to which FACTS solutions are most directly applicable are stability related. These can be further delineated into the sub-headings of transient stability, ambient damping, voltage stability and subsynchronous resonance instability.

Transient stability describes the ability of a power system to retain synchronism for the initial few seconds after a major disturbance, where full-range response of controllers is dominant. A typical measure of performance is to ensure all post-fault voltages remain above approximately 80 percent of the nominal voltage level during the subsequent system swings [3].

Where transient stability has been a limiting constraint in the past, a number of approaches have been taken to improve the performance including the use of [3]:

- Series capacitors, both continuously in operation or mechanically-switched
- High-response excitation systems on major generators
- Remedial action schemes such as generator tripping or controlled separation
- Rapid switching of a braking resistor (using mechanical switchgear)
- Rapid switching of shunt capacitor banks (using mechanical switchgear)

If a system is well damped it is said to have "ambient damping," this means that all power-swing oscillations will decay once initiated by any small disturbance. Typically, limits are set either by establishing a time to half the oscillatory decay, or by determining the power transfer at which no damping exists and choosing a lower transfer to provide an operating margin.

Approaches which have been used to improve ambient damping include [3]:

- Power system stabilizer (PSS) on generator excitation systems. These have been applied in many parts of the world since the 1960's.
- Modulation controls on HVDC systems. These are a powerful means of aiding damping, but are applied in only a few projects.
- Modulation control on static var compensators (SVC) systems. This may be helpful if the SVC is in a suitable location, but again it is applied to only a few schemes.

The voltage stability limit when applied to power systems describes the situation when the next increment of load causes a voltage collapse. This voltage reduction is generally a slow decay, occurring over time periods ranging form many seconds to minutes.

Voltage collapse is becoming more prevalent as a constraint on power transfer and to date has been addressed by [3]:

- Operator actions, monitoring voltage and comparing it to experience-based criteria and re-dispatching or restricting power flow on highly-stressed lines.
- Adding series compensation to key lines. This has been found to be a very effective solution in many bulk power transmission cases.
- Adding more voltage strengthening equipment, such as generators or synchronous condensers.

- Voltage controlling equipment such as SVCs.

Another limitation, which may be considered a stability issue, is due to interactions between the AC power transmission system and torsional vibration modes of turbine-generator units. Most situations where this issue constrains operating conditions exist when the interactions are related to series compensated AC lines. In this context, the phenomenon is referred to as "subsynchronous resonance" (SSR). This SSR issue is typically addressed by constraining the level of series compensation permitted in key lines to ensure safe operation, considering extreme contingencies as well as normal operation. Often this safe level of series compensation is below that desired for power system security at the otherwise attainable power transfer levels. Other approaches for alleviating SSR have included:

- Bypass of series capacitors during unstable operation (transfer-trip schemes)
- Passive series blocking filters
- Active control via generator excitation modulation
- Active control using a large SVC on the generator bus

With any application where SSR might be an issue, generator-based protection is usually applied to cover unexpected contingencies. The key issue is that the electrical impedance must be such that, when a shaft torsional oscillation mode is stimulated, the changes in electrical torque due to this shaft oscillation must not be in a direction that significantly decreases the net damping of the oscillation.

1.1.3.2 Voltage limits

Voltage control is accomplished in conventional systems by a combination of generator reactive power adjustment, fixed or mechanically switched shunt reactors or capacitors and mechanical tap changers on transformers. Shunt reactive equipment is used for

coarse control, while the generators (or rotating synchronous condenser) provide vernier control of voltage. It has been shown that power electronic controllers can aid in voltage control, acting as a vernier adjustment or giving a fast response to transients [3].

1.1.3.3 Thermal overload limits

Thermal limits are inherent in transmission systems, due to both conductor limits and series equipment such as transformers, reactors, or series capacitors. Transmission lines are generally operated at levels so as to provide security in the event of a major disturbance. The role of controllers will be to affect the operation of the system, usually in response to the disturbances of concern, permitting increased utilization of this thermal capacity.

1.1.4 Power flow control

As stated in section 1.1.1, a second objective of FACTS development is to provide direct control of power flow over designated transmission routes.

In tightly meshed networks, incidents like the loss of a line do not generally endanger the stability of the system. However these events can cause unacceptably high voltage drops and/or the overload of parallel paths if the initial loading of the lost line is sufficiently high. These voltage drops and overloads are the most widespread causes of transmission limitations.

Power flow control has traditionally relied mostly on control of generators, network switching, and phase shifting transformers. It is anticipated that power electronic controllers will be used to augment the traditional means, primarily by supplying smooth control under steady-state conditions or frequent operations and improved performance for post-contingency conditions.

1.2 Solutions to limitations by using FACTS

The purpose of this section is to discuss solutions to the transmission system limitations outlined in the previous section. The primary benefit of FACTS controllers is the rapid control of current, voltage and/or impedance following disturbances. Thus, an important expectation of FACTS controllers is a reduction of the primary disturbance impact.

1.2.1 Steady-state issues

Table 1.1 summarizes FACTS solutions for steady-state issues. Two of the principal causes of steady-state transmission limitations are high or low voltage, and thermal capabilities of lines and equipment [2]. Generally, FACTS controllers are not required to correct steady-state limitations. However, if action must be implemented quickly (e.g., post-contingency), a FACTS controller may be advantageous.

1.2.2 Dynamic issues

The dynamic behavior aspects of transmission systems that can be improved with the use of FACTS controller include transient stability, damping oscillations and voltage stability. Again, from the both planning and operating points of view, one of the most important benefits expected of FACTS applications is to be able to reduce the impact of the primary disturbance [2]. This not only improves the use of transmission capability but also makes the network more capable of handling a second incident and thus helps prevent subsequent cascading failures [2]. This impact reduction for contingencies can be achieved through dynamic voltage support (STATCOM), dynamic flow control (TCPAR and TCSC) or both the UPFC and IPC (with power electronics) [2]. Table 1.2 summarized FACTS solutions for dynamic issues [2].

Table 1.1 Steady state issues

Issue	*Problem*	*Corrective action*	*FACTS solutions*
Voltage limits	Low voltage at heavy load	Supply reactive power	TCSC[a], SVC[b], STATCOM[c]
	High voltage at light load	Remove reactive power supply	TCSC, TCR[d]
		Absorb reactive power	TCR, STATCOM
	High voltage following outage	Absorb reactive power	TCR
		Protect equipment	TCVL[e]
	Low voltage following outage	Supply reactive power	STATCOM, TCSC
		Prevent overload	IPC[f], TCPAR[g], TCSC
	Low voltage and overload	Supply reactive power and limit overload	TCSC, UPFC[h], STATCOM
Thermal limits	Line/transformer overload	Reduce overload	TCSC,TCPAR, UPFC
	Tripping of parallel circuit	Limit circuit loading	IPC, UPFC, TCR

[a]TCSC = Thyristor Controlled Series Capacitor
[b]SVC = Static Var Compensators
[c]STATCOM = Static Synchronous Compensator
[d]TCR = Thyristor Controlled Reactor
[e]TCVL = Thyristor Controlled Voltage Limiter
[f]IPC = Interphase Power Controller
[g]TCPAR = Thyristor Controlled Phase-angle Regulator
[h]UPFC = Unified Power Flow Controller

1.3 Brief description of TCSC

Increased loads and higher inter-area power transfer, coupled with declining construction of new transmission lines have increased the risk of poorly damped oscillations in the range of 0.1 to 0.8 Hz. Power system stabilizers (PSS) are commonly used to increase the damping of swing modes. Shunt var controllers (SVC) have been used to damp the inter-area and local electro-mechanical oscillation modes. With the appearance of high power thyristors, there has been a great interest in using TCSC in transmission lines for the dual purpose of altering the steady-state power flow and enhancing power system stability. This interest is based on the idea that control of transmission line reactance can significantly change system modal behavior.

Power transfer between areas can also be affected by adjusting the net series impedance.

Table 1.2 Dynamic issues

Issue	*Type of system*	*Corrective action*	*FACTS solutions*
Transient stability	A[a],B[b],D[c]	Increase synchronizing torque	TCSC, UPFC
	B,C[d],D	Dynamic flow control	TCPAR,UPFC, TCSC
Damping	A	Damp 1 Hz oscillations	TCSC, STATCOM
	B,D	Damp low frequency oscillations	SVC,TCPAR, UPFC, TCSC,STATCOM
Post-contingency voltage control	A,B,D	Dynamic voltage support	STATCOM, UPFC,SVC
		Dynamic flow control	STATCOM, UPFC
		Dynamic voltage support and flow control	UPFC, TCSC,SVC
	A,B,C,D	Reduce impact of contingency	TCSC,STATCOM, IPC,UPFC
Voltage stability	B,C,D	Reactive support	STATCOM, UPFC
		Network control actions	UPFC,IPC, TCSC,STATCOM
		Load control	Demand-side management programs

[a]A. Remote generation - radial lines
[b]B. Interconnected areas
[c]D. Loosely meshed network
[d]C. Tightly meshed network

One such established method of increasing transmission line capability is to install a series capacitor which reduces the net series impedance, thus allowing additional power to be scheduled. This method is well known and comes under the heading of series compensation [3]. Three methods of series capacitor control have been developed and implemented [6]:

- Mechanically switched series capacitors (MSSC).
- Thyristor switched series capacitors (TSSC).
- Thyristor controlled series capacitors (TCSC).

Conventional series compensation schemes switch capacitors to vary the level of com-

pensation by use of mechanical devices such as power circuit breakers. The limitations of using mechanical switching devices force conventional series compensation schemes to be switched in relatively large discrete segments with relatively slow switching times [3]. Thyristor controllers however are able to rapidly control the line compensation over a continuous range with resulting flexibility. Therefore, the second method of switching series capacitors employs thyristors as the switching elements rather than mechanical devices. This has the advantage of providing greater speed in switching.

The third method of controlling series compensation that has been implemented is the thyristor controlled series capacitor (TCSC). In this scheme, an inductance is placed in parallel with the series capacitor, and the current through the inductor is controlled.

One application of the TCSC concept is shown in Figure 1.1 [6]. This application of thyristors is unique and considerably different from other applications, such as HVDC and SVC systems. TCSC controllers use thyristor controlled reactors (TCR) in parallel with capacitor segments (C) of a series capacitor bank. This combination allows the capacitive reactance to be smoothly controlled over a wide range and switched upon command to a condition where the bidirectional thyristor pairs conduct continuously (full cycle) and insert an inductive reactance into the line [3]. Another type of TCSC system that has been constructed is the so-called Advanced Series Compensation (ASC) system [7]. This system also uses a thyristor controlled reactor that is in parallel with a segment of the series capacitor, as shown in Figure 1.2 [6]. The series capacitor bank shown in the figure consists of a common series capacitor with varistor bypass in series with the ASC system.

In some applications, a relatively smooth control of reactance will be needed to securely damp power swings or to regulate power flow on adjacent paths. Such applications will likely need this smooth control at times of high system stress, where the lines with TCSC are likely to carry more than their continuous current rating [3]. Dividing a TCSC into multiple segments is a practical and economical means of achieving such a

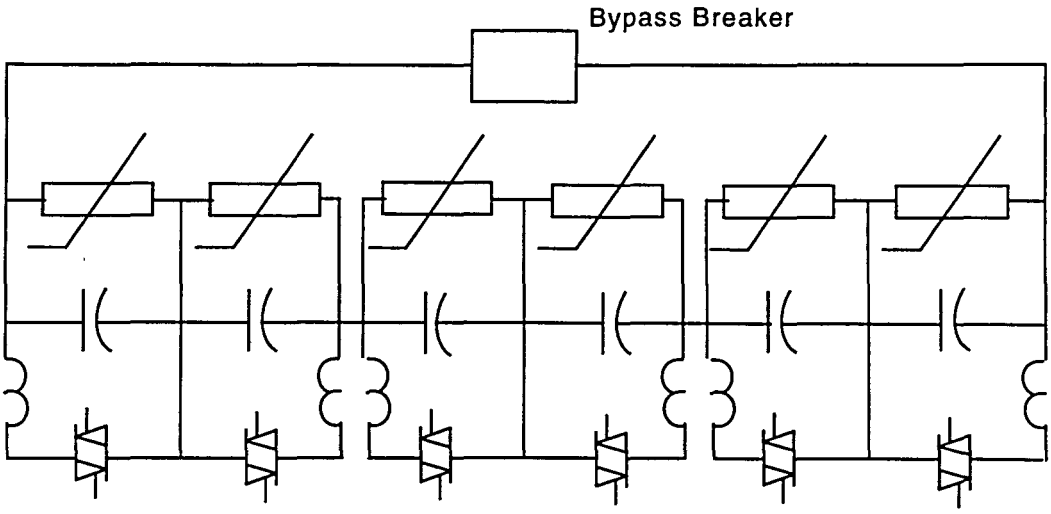

Figure 1.1 Structure of the TCSC

characteristic. In fact, the more modules into which the TCSC is divided, the greater the usable control range [3].

Network power swing damping capability can be provided by TCSC. Damping is achieved by dynamically modulating the power flow to reduce the system oscillations. TCSCs also allow higher levels of series compensation with significantly reduced risk of SSR interaction [3].

1.4 Problem statement

Much industry effort is presently being devoted to exploitation of the concept of variable series compensation in AC transmission networks made possible by breakthroughs in power electronics. One obvious motivation for using variable or controlled compensation is to make possible increased utilization of particular transmission corridors that cause undesired changes in loading of parallel paths. These benefits of controlled compensation can be assessed from a steady state viewpoint, with the control characteristics being dictated mainly by dynamics of dispatch and system load change rates as well as contin-

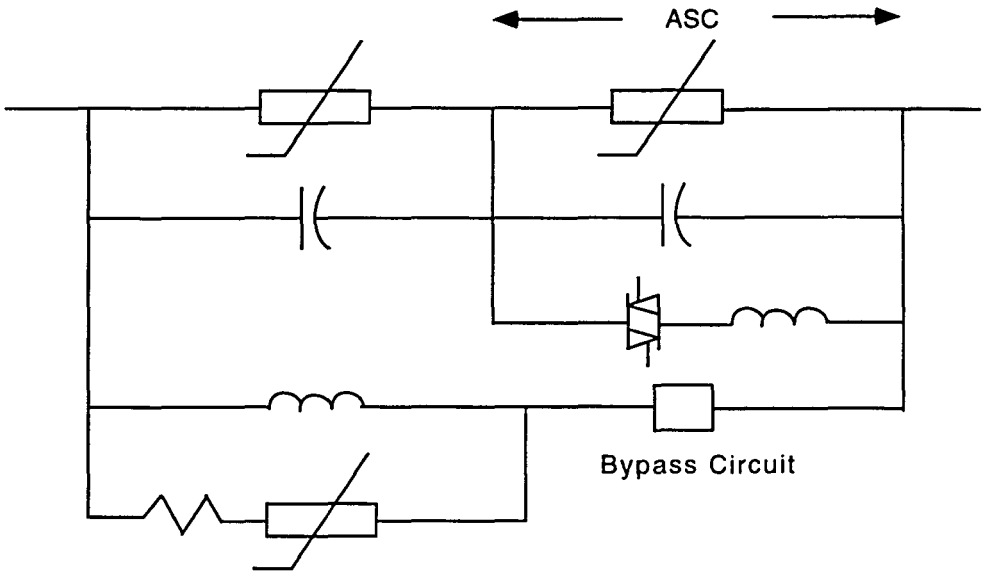

Figure 1.2 Advanced series capacitor concept

gency considerations. Another possible benefit of continuously adjustable compensation is to use it to improve the damping of electro-mechanical oscillations characteristic of power systems. The damping of such oscillations is often the limiting factor to loading or power transfer of transmission systems.

TCSC is one of the FACTS devices which improves the power system stability by appropriately controlling the effective reactance of transmission lines. The hardware designs for TCSCs have been well established under an Electric Power Research Institute (EPRI) project for FACTS application [8, 9, 10]. Extensive investigations on the design of TCSC controllers have been carried out. Previous research has shown the effectiveness of TCSC controllers on increasing the damping of low frequency inter-area oscillations [11]. Also, as it has been shown in [12], the contribution of TCSC to damping of local modes is always positive and TCSC exhibits more effective damping than SVC for inter-area modes. Although the improvement of damping is more cost effective with the application of PSS, in cases where other considerations dictate the installation of continuously controlled series compensation, the use of appropriate control intelligence

can yield important damping benefits [13].

For a meshed power system, the selection of the transmission line on which the TCSC is to be installed is very important because the effectiveness of TCSC control varies with the TCSC installation location. If the objective of the TCSC control design is to increase the damping of the dominant oscillation modes without significantly deteriorating the damping of the other oscillation modes, then one of the important aspects of designing a TCSC controller for a multi-machine power system is to identify the most effective TCSC location for required control objective which can be providing additional damping to a particular swing mode. In this thesis, the most effective location is determined through eigenvalue sensitivity analysis.

1.5 Thesis organization

The thesis is organized as described here. Small signal stability problems are reviewed in Chapter 2. Power system modeling is discussed in Chapter 3. Modal sensitivity analysis in transmission systems is discussed in Chapter 4. Chapter 5 gives a numerical example for the above sensitivity methods. Conclusions and suggestions for future work are discussed in Chapter 6.

2 SMALL SIGNAL STABILITY IN POWER SYSTEMS

In the early days of interconnected power systems, the instability of greatest concern between interconnected generators was loss of synchronism monotonically in the first few seconds following a fault. This type of instability is due to lack of synchronizing torque and is essentially caused by the non-linear nature of the dynamics of interconnected generators. Automatic voltage regulators (AVRs), operating through the generator's excitation systems, have the effect of increasing the synchronizing torques between interconnected generators. However, they have the secondary effect of reducing the damping torques and make the system more prone to oscillatory instability. This type of instability is amenable to analysis via linear system theory. The use of special techniques for linear dynamic analysis, applied to linearized system models, gives information on both the nature of oscillatory instability and on controls which can be used to eliminate instability [14]. This method is called small signal stability analysis. In this chapter, the small signal stability method and its application in analysis of power system electro-mechanical modes is discussed.

2.1 Small signal stability

Small signal stability is the ability of the power system to maintain synchronism when subjected to small disturbances. A disturbance is considered to be small if the equations that describe the dynamics of the power system may be linearized for the purpose of analysis. The instability that may result can be of two forms: (i) steadily increasing

generator rotor angle due to lack of synchronizing torque, or (ii) rotor oscillations of increasing amplitude due to lack of sufficient damping torque. The latter problem is typically amenable to small signal analysis. Small signal analysis using linear techniques provides valuable information about the inherent dynamic characteristics of the power system and assists in its design [14].

2.2 Eigenproperties of state matrix

The essential dynamical characteristics of a linear time-invariant system (LTI) of the type

$$\dot{X} = AX + BU \tag{2.1}$$

are expressed in terms of the eigen-properties of the matrix A.

2.2.1 Eigenvalues and eigenvectors

The eigenvalues of a matrix A are given by the values of the scalar parameter λ for which there exist non-trivial solutions (i.e., other than $\Phi = 0$) to the equation

$$A\Phi = \lambda\Phi \tag{2.2}$$

where A is an $n \times n$ matrix (real for a physical system such as a power system) and Φ is an $n \times 1$ vector

For any eigenvalue λ_i, the n-column vector Φ_i which satisfies Equation (2.2) is called the right eigenvector of A associated with the eigenvalue λ_i. Therefore, we have:

$$A\Phi_i = \lambda_i\Phi_i, \qquad i = 1, 2, ..., n \tag{2.3}$$

Similarly, the n-row vector Ψ_i which satisfies

$$\Psi_i A = \lambda_i\Psi_i, \qquad i = 1, 2, ..., n \tag{2.4}$$

is called left eigenvector of A associated with the eigenvalue λ_i.

2.2.2 System modes and Lyapunov's first method

2.2.2.1 System modes

In the absence of an input, the state equation of the linear time invariant system assumes the form

$$\dot{X}(t) = AX(t) \tag{2.5}$$

where A is a real $n \times n$ matrix and $X(t)$ is an $n \times 1$ state vector whose variation with time defines the free motion of the system. The precise nature of the free motion of the linear time-invariant system (LTI) following any disturbance can be described in terms of the eigenvalues and eigenvectors of the matrix A.

The equation describing the free motion of the system (2.5) can be expressed in the form

$$X(t) = \sum_{i=1}^{n} [\exp \lambda_i t]\ \phi_i \psi_i X(0) \tag{2.6}$$

Equation(2.6) shows clearly that the free motion of the linear-time invariant system governed by (2.5) is a linear combination of n functions of the form $[\exp \lambda_i t]\phi_i$, $(i = 1, 2, ..., n)$ which are said to describe the n dynamical modes of the system. Thus, the shape of a mode is described by its associated eigenvector, ϕ_i, and its time-domain characteristics by its associated eigenvalue, λ_i. It is evident from (2.6) that the equilibrium state $X = 0$ of the system (2.5) will be asymptotically stable in the sense that $X(t) \to 0$ as $t \to \infty$ if and only if

$$Re\lambda_i < 0, \qquad i = 1, 2, ..., n \tag{2.7}$$

2.2.2.2 Lyapunov's first method

The stability in the small of a nonlinear system is given by the roots of the characteristic equation of the system of first approximations, i.e., by the eigenvalues of system A matrix[14]:

- When all eigenvalues have negative real parts, the original system is asymptotically stable.
- When at least one of the eigenvalues has a positive real part, the original system is unstable.
- When at least one of the eigenvalues have real parts equal to zero, with all other eigenvalues having negative real parts, then it is not possible on the basis of the first approximation to tell whether the system is stable or unstable.

2.2.3 Mode shape, participation factor

2.2.3.1 Mode shape

Right eigenvector gives the mode shape, i.e., the relative activity of the state variables when a particular mode is excited. For example, the element Φ_{ki} of the right eigenvector Φ_i gives the degree of activity of the state variable x_k in the ith mode[14].

2.2.3.2 Participation factor

One problem in using right and left eigenvectors individually for identifying the relationship between the states and the modes is that the elements of the eigenvectors are dependent on units and scaling associated with the state variables. As a solution to this problem, a matrix called the participation matrix (P), which combines the right and left eigenvectors, is used as a measure of the association between the state variables and the modes [14]. The element

$$p_{ki} = \phi_{ki}\psi_{ik} \tag{2.8}$$

is termed the participation factor. It is a measure of the relative participation of the kth state variable in the ith mode, and vice versa.

2.2.4 Relationship between eigenproperties and transfer functions

The state-space representation is concerned not only with input and output properties of the system but also with its complete internal behavior. In contrast, the transfer function representation specifies only the input/output behavior. Hence, one can make an arbitrary selection of state variables when a plant is specified only by a transfer function. On the other hand, if a state-space representation of a system is known, the transfer function is uniquely defined. From this point of view, the state-space representation is a more complete description of the system; it is ideally suited for the analysis of multi-variable multi-input and multi-output systems [14].

For small signal stability analysis of power systems, we primarily depend on the eigenvalue analysis of the system state matrix. However, for control design we are interested in an open-loop transfer function between specific variables. To see how this is related to the state matrix and to the eigenproperties, let us consider the transfer function between the variables y and u.

$$\Delta\dot{x} = A\Delta x + b\Delta u \tag{2.9}$$

$$\Delta y = c\Delta x + d\Delta u \tag{2.10}$$

where A is the state matrix, Δx is the state vector, Δu is a single input, Δy is a single output, c is a row vector and b is a column vector. We will assume that y is not a direct function of u (i.e., d=0). We also assume that A has distinct eigenvalues.

The required transfer function can be found from the Laplace transforms of (2.10) and (2.10) and is

$$\begin{aligned} G(s) &= \frac{\Delta y(s)}{\Delta u(s)} \\ &= c(sI - A)^{-1}b \end{aligned} \tag{2.11}$$

This has the general form

$$G(s) = K\frac{N(s)}{D(s)} \tag{2.12}$$

After factorization of $D(s)$ and $N(s)$, we may write

$$G(s) = K\frac{(s-z_1)(s-z_2)...(s-z_l)}{(s-p_1)(s-p_2)...(s-p_n)} \tag{2.13}$$

Now, $G(s)$ can be expanded in partial fractions as

$$G(s) = \frac{R_1}{(s-p_1)} + \frac{R_2}{(s-p_2)} + ... + \frac{R_n}{(s-p_n)} \tag{2.14}$$

and R_i is known as the *residue* of $G(s)$ at pole p_i.

To express the transfer function in terms of the eigenvalues and eigenvectors, we express the state variables Δx in terms of the transformed variables z defined by

$$\Delta x = \Phi\, z \tag{2.15}$$

Thus, we have

$$\begin{aligned} \dot{z} &= \Phi^{-1}A\Phi z + \Phi^{-1}b\Delta u \\ &= \Lambda z + \Phi^{-1}b\Delta u \end{aligned} \tag{2.16}$$

and

$$\Delta y = c\ \Phi\ z \tag{2.17}$$

From the Laplace transforms of (2.16) and (2.17), we may write

$$\begin{aligned} G(s) &= \frac{\Delta y(s)}{\Delta u(s)} \\ &= c\Phi[sI-\Lambda]^{-1}\Psi b \end{aligned} \tag{2.18}$$

Since Λ is a diagonal matrix with distinct eigenvalues,

$$G(s) = \sum_{i=1}^{n}\frac{R_i}{(s-\lambda_i)} \tag{2.19}$$

where

$$R_i = c\ \Phi_i\ \Psi_i\ b \tag{2.20}$$

2.3 Sensitivity analysis method

2.3.1 Eigenvalue sensitivity to a certain parameter

Let us examine the sensitivity of eigenvalues to a certain parameter p.

$$A\phi_i = \lambda_i \phi_i \tag{2.21}$$

Differentiating with respect to p yields:

$$\frac{\partial A}{\partial p}\phi_i + A\frac{\partial \phi_i}{\partial p} = \frac{\partial \lambda_i}{\partial p}\phi_i + \lambda_i \frac{\partial \phi_i}{\partial p} \tag{2.22}$$

Premultiplying by ψ_i, and noting that $\psi_i(A - \lambda_i I) = 0$, we see that the above equation simplifies to

$$\frac{\partial \lambda_i}{\partial p} = \frac{\psi_i \dfrac{\partial A}{\partial p}\phi_i}{\psi_i \, \phi_i} \tag{2.23}$$

2.3.2 Functional sensitivity

In Figure 2.1, $G(s)$ is a transfer function relating the variables $u(s)$ and $y(s)$ between which it is desired to close a feedback $H(s,k) = k\ h(s)$, where k is a scalar and $h(s)$ is of a specified structure. Assuming that all the zeros and poles of $G(s)$ and $H(s)$ are distinct, it has been shown in [15, 16] that for small values of k, the closure of the feedback loop causes a change in λ_i given by:

$$\frac{\partial \lambda_i}{\partial k} = \frac{\partial H(\lambda_i)}{\partial k} R_i \tag{2.24}$$

$$\Rightarrow \Delta\lambda_i = R_i H(\lambda_i) \tag{2.25}$$

where λ_i is a pole of $G(s)$ and R_i is its associated residue. This property, as suggested in [15], can be used to shift the poles (system eigenvalues) associated with the electro-mechanical oscillations with reduced damping. It lays the foundation of a useful

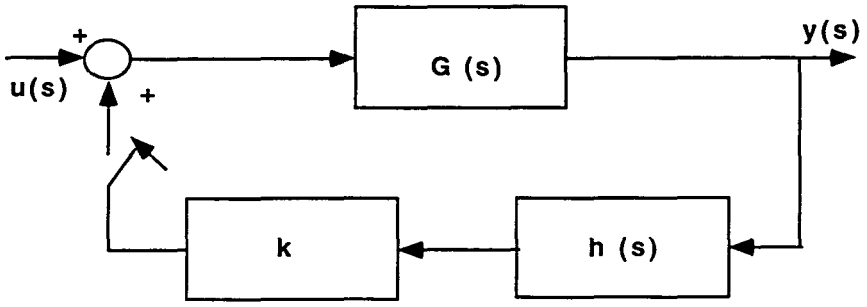

Figure 2.1 Transfer function

conceptual, as well as algorithmic, separation of the effect of the feedback location (which determines R_i) and the effect of the parameter k [16]. If we interpret the sensitivity as the shift introduced on the eigenvalue by a unitary increment of a real gain k, we can see from (2.25) that by shaping the phase of $\Delta\lambda_i$ through $H(\lambda_i)$, it is possible to orient the shift in a desired direction; and then the amount of shift will be adjusted by the magnitude of k [16]. The residue R_i in (2.25) can be evaluated from the forward loop ($G(s)$) if the feedback is a new addition to the system (i.e., $H(s) = 0$ for the nominal value of k).

2.4 Special techniques for analysis of very large power systems

Analysis of inter-area oscillations in a large interconnected power system requires detailed modeling of the entire system. System representations with up to 2,000 dynamic devices and 12,000 buses are sometimes required for such studies. With as many as 15 states per device, the number of state variables required for modal analysis may thus be on the order of 30,000. This is well outside the range of the conventional eigenvalue analysis methods. Special techniques have been developed that focus on evaluating a

selected subset of eigenvalues associated with the complete system response[14].

- The AESOPS (Analysis of Essentially Spontaneous Oscillations in Power Systems) algorithm uses a novel frequency response approach to calculate the eigenvalues associated with the rotor angle modes.

- SMA (Selective Modal Analysis) approach computes eigenvalues associated with selected modes of interest by using special techniques to identify variables that are relevant to the selected modes and then constructing a reduced-order model that involves only the relevant variables.

- Modified Arnoldi and simultaneous iterations methods are sparsity-based eigenvalue techniques.

The PEALS (Program for Eigenvalue analysis of Large Systems) uses two of these techniques: the AESOPS algorithm and the modified Arnoldi method.

2.5 Characteristics of small-signal stability problems

In large power systems, the small-signal stability problems may be either local or global in nature [14].

2.5.1 Local problems

Local problems may be associated with rotor angle oscillations of a single generator or a single plant against the rest of the power system. Such oscillations are called local plant mode oscillations. Local problems may also be associated with oscillations between the rotors of a few generators close to each other. Such oscillations are called inter-machine or inter-plant mode oscillations.

2.5.2 Global problems

Global problems are caused by interactions among large groups of generators and have widespread effects. They involve oscillations of a group of generators in one area swinging against a group of generators in another area. Such oscillations are called *inter-area mode oscillations.* Large interconnected systems usually have two distinct forms of inter-area oscillations:

- A very low frequency mode involving all the generators in the system. The system is essentially split into two parts, with generators in one part swinging against machines in the other part. The frequency of this mode of oscillation is on the order of 0.1 to 0.3 Hz.

- Higher frequency modes involving subgroups of generators swinging against each other. The frequency of these oscillations is typically in the range of 0.4 to 0.7 Hz.

2.6 Determination of location of PSS

In this section, we review methods used for PSS siting problem. Power system stabilizers are used as an additional control feature in order that excitation systems with high response may be used without compromising the small signal instability of the generators rotor angle mode. For damping enhancement of the poorly damped modes, it is common to use PSS with local rotor-speed input signal at different machines. The most effective generators for installing PSSs are determined by using participation factors (PF) or transfer function residues [17].

2.6.1 Location of PSS using PF

Participation factor indicates how much a certain state participates in a certain mode. The participation of state k in the ith mode is given by equation (2.8). The machines

with highest PF in the mode of interest are good candidates for applying control via PSS.

2.6.2 Location of PSS using residues

This method is based on transfer function residues which provide a measure of controllability and observability of these modes from different areas or stations. First-order residues have been used for PSS siting and phase compensation. Large magnitudes of residues imply that small PSS gains are needed. Phase information of residues is also important. A good station candidate for PSS [18] :

- should have all large first-order residues of critical modes bundled in a cone with a narrow angle ($< \pi/2$)
- should remain large in magnitudes
- should have all large first-order residues of critical modes bundled for different operating conditions.

In this way, even if the frequencies of critical modes are close to each other, when one residue vector is turned towards the negative real axis by a PSS, the others will not be moved to the right-half complex plane, i.e., stabilization of one mode will not destabilize another.

It is convenient to choose $G^k(s)$, where $k = 1, 2, ..., Ng$, (Ng is the number of generators in the system), as the transfer function between the reference voltage of the automatic voltage regulator (V_{ref}) and a measurable variable (y) from which the power system stabilizer is derived. Therefore, the machines with highest $R_i = c\ \psi_i \phi_i\ b$ in the mode of interest are good candidates for applying control via PSS.

2.7 TCSC siting methods

TCSC is a new control device used in power system compared to PSS. Two methods have already been proposed to determine the location for TCSC. They are (1) controllability method and (2) transfer function residues method.

In the first method the three longest transmission lines in the study system are assumed to be the possible TCSC locations, and three case studies are carried out in order to evaluate the effectiveness of the TCSCs placed at these locations in the power system. This task is accomplished by analyzing the mode controllability of the system. The magnitude of $\Phi^{-1}B$ is used to indicate the controllability of the corresponding modes (Φ is the modal matrix) [19]. The TCSC reactance is selected as a state variable in this method [19].

The second method used the residue ranking list of transfer functions $\frac{\Delta P_{line}(\lambda)}{\Delta B_{line}(\lambda)}$, $line = 1, ..., Nl$ (Nl being the total number of lines in the system) to help determine the most effective lines to place a Thyristor Controlled Series Capacitors to damp a certain mode [20].

The first method asks for a description of TCSC controller and models it in the system matrix; the second method requires specification of input and output signals for the controller. Both methods use some information about the controller such as input signal, control law, etc.

In this research, two methods of sensitivity analysis are carried out determine the TCSC effectiveness. One of them is parameter sensitivity with respect to the line susceptance method. In contrast to the above mentioned two methods, this method does not need any information about controller design. The other method is functional sensitivity which is also called the residue method.

3 SYSTEM MODELING

Analysis of inter-area oscillations requires detailed representation of the entire interconnected power system. The characteristics of inter-area modes of oscillation are very complex and in some respects significantly differ from the characteristics of local plant modes. Load characteristics, in particular, have a major effect on the stability of inter-area modes. The manner in which excitation systems affect inter-area oscillations depends on the types and locations of the exciters, and on the characteristics of loads. Speed-governing systems normally do not have a very significant effect on inter-area oscillations. In this chapter, the mathematical models of power system elements such as the generator model, load model, and exciter model along with overall representation of the power system are discussed.

3.1 Structure of the power system

Electric power systems vary in size and structural components. However, they all share some basic characteristics, among which are the following [14]:

- They are comprised of three-phase AC systems operating essentially at constant voltage. Generation and transmission facilities use three-phase equipment. Industrial loads are invariably three-phase; single-phase residential and commercial loads are distributed equally among the phases so as to effectively form a balanced three-phase system.

- They use primarily synchronous machines for generation of electricity. Prime movers convert the primary sources of energy (fossil, nuclear, and hydraulic) to mechanical energy that is, in turn, converted to electrical energy by synchronous generators.

- They transmit power over significant distances from the generators to consumers. This requires a transmission system typically comprised subsystems operating at different voltage levels.

Analysis of practical power systems involves the simultaneous solution of equations representing the following [14]:

- Synchronous machines, and the associated excitation systems and prime movers
- Interconnecting transmission network
- Static and dynamic (motor) loads
- Other devices such as HVDC converters, and static var compensators

3.2 Generator modeling

When the effects of excitation are included in power system dynamic analysis, the simplest model of a generator is a third order model [21]. This is the model used in this work.

This practical model is derived based on the following assumptions [5]:

- The subtransient effects are neglected
- In the stator voltage equations the terms $p\Phi_d = p\Phi_q = 0$; i.e., $p\Phi_d$ and $p\Phi_q$ are negligible compared to the speed voltage terms
- $\omega \approx \omega_R = 1 \quad p.u.$

- D, Q winding are neglected

It is called the one axis model because this model neglects amortisseur effects and $p\Phi_d$ and $p\Phi_q$ terms [5].

3.2.1 State equations of generator

The state equation for the three state, one axis model of a synchronous generator are as follows:

$$T'_{d0i}\dot{E}'_{qi} = E_{FDi} - E'_{qi} - I_{di}(x_{di} - x'_{di}) \tag{3.1}$$

$$T_{ji}\dot{w}_i = M_{Ti} - M_{ei} - D_i * (w_i - 1) \tag{3.2}$$

$$\dot{\delta}_i = 2\pi f_0(\omega_i - 1) \tag{3.3}$$

where

ω_i in pu;

δ_i in rad;

$T_{ji} = 2H$ in sec;

$Td0'_i$ in sec;

others in pu.

3.2.2 Voltage equations for generator stators

The equation relating the internal and terminal voltages are

$$E'_{qi} = V_{qi} + I_{di}\ x_{di}' \tag{3.4}$$

$$0 = V_{di} - I_{qi}\ x_{qi} \tag{3.5}$$

The equations are necessary for computing the currents. From the above equations, we have:

$$I_{di} = \frac{E'_{qi} - V_{qi}}{x'_{di}} \tag{3.6}$$

$$I_{qi} = \frac{V_{di}}{x_{qi}} \tag{3.7}$$

Note that in the one axis machine model, $x_{qi} = x'_{qi}$.

3.2.3 Generator's electric power

The power supplied at the generator terminals to the rest of the network is given by:

$$\begin{aligned} P_{Ei} + jQ_{Ei} &= \dot{V}_i \dot{I}_i^* \\ &= (V_{di} + jV_{qi})(I_{di} - jI_{qi}) \\ &= (V_{di}I_{di} + V_{qi}I_{qi}) + j(V_{qi}I_{di} - V_{di}I_{qi}) \end{aligned}$$

so:

$$P_{Ei} = V_{di}I_{di} + V_{qi}I_{qi} \tag{3.8}$$

$$Q_{Ei} = V_{qi}I_{di} - V_{di}I_{qi} \tag{3.9}$$

3.2.4 Machine network interface

Each machine model is expressed in its own $d-q$ reference frame which rotates with its rotor. For the solution of interconnecting network equations, all voltages and currents must be expressed in a common reference frame. Usually a reference frame rotating at synchronous speed is used as the common reference. Axis transformation equations are used to transform between the individual machine $(d-q)$ reference frames and the common $(D-Q)$ reference frame as shown in Figure 3.1.

$$V_{di} = V_{Di}\sin(\delta_i - \theta_i) \tag{3.10}$$

$$V_{qi} = V_{Qi}\cos(\delta_i - \theta_i) \tag{3.11}$$

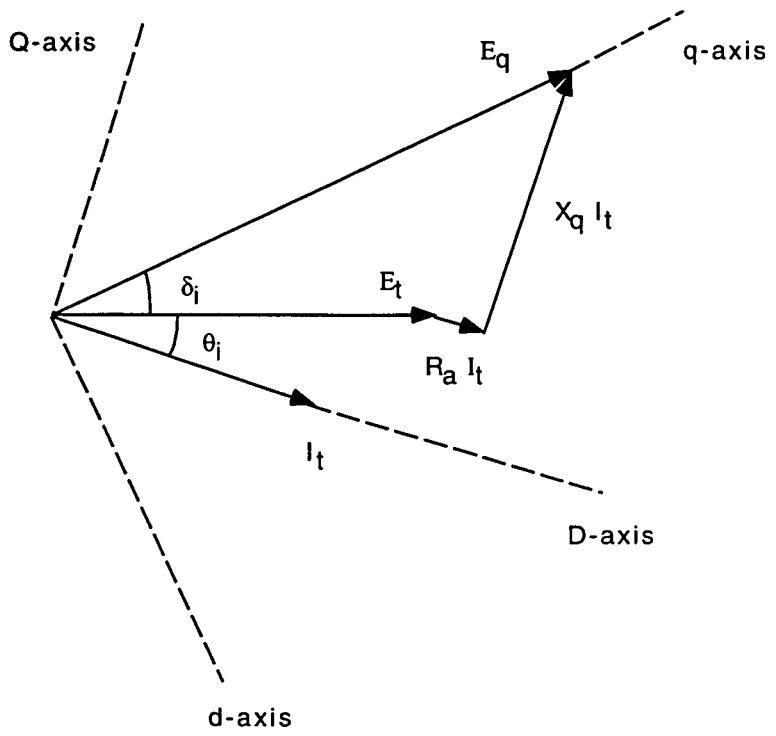

Figure 3.1 Machine and network interface

3.2.5 Initial value calculation

Since we have:

$$\begin{aligned} V_i &= V_{Di} + jV_{Qi} \\ I_i &= I_{Di} + jI_{Qi} \\ S_i &= V_i \, \dot{I}_i^* \end{aligned}$$

then:

$$I_i = \frac{S_i^*}{\dot{V}_i^*} \tag{3.12}$$

From Figure 3.1, we have:

$$\begin{aligned} \tilde{E_{qi}} &= V_i + I_i(R_{ai} + jx_{qi}) \\ &= \tilde{E}_{qDi} + j\tilde{E}_{qQi} \end{aligned}$$

then, we get:

$$\delta_i = \arctan \frac{\tilde{E}_{qDi}}{\tilde{E}_{qQi}} \tag{3.13}$$

Since

$$\omega_i = 1 \tag{3.14}$$

and

$$\begin{aligned} V_{di} &= \sin(\delta_i)V_{Di} - \cos(\delta_i)V_{Qi} \\ V_{qi} &= \cos(\delta_i)V_{Di} + \sin(\delta_i)V_{Qi} \end{aligned} \tag{3.15}$$

$$\begin{aligned} I_{di} &= \sin(\delta_i)i_{Di} - \cos(\delta_i)I_{Qi} \\ I_{qi} &= \cos(\delta_i)i_{Di} + \sin(\delta_i)I_{Qi} \end{aligned} \tag{3.16}$$

Also, we have

$$E_{qi}^{'} = V_{qi} + I_{di}x_{di}^{'} \tag{3.17}$$

$$E_{FDi} = E_{qi}^{'} + I_{di}(x_{di} - x_{di}^{'}) \tag{3.18}$$

3.3 Exciter modeling

A model structure for a typical exciter is shown in Figure 3.2 [21]. After simplification, the state equation for the exciter is:

$$(T_{Ai} + T_{ei})\dot{E}_{FDi} = -E_{FDi} + K_{Ai}K_{ei}(V_{refi} - V_i) \tag{3.19}$$

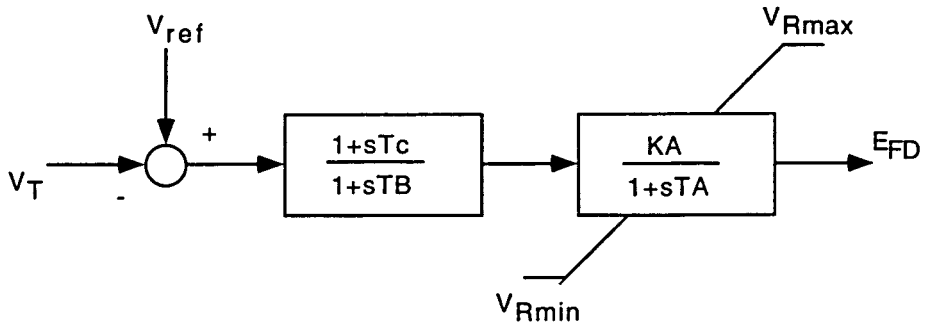

Figure 3.2 Model for typical exciter

3.4 Load modeling

As equation (3.2) indicates, stable operation of a power system following a disturbance depends on the instantaneous power supplied by each generator, which in turn depends on the dynamics of the load. Consequently, load characteristics have an important influence on system stability.

The modeling of loads is complicated because a typical load bus represented in stability studies is composed of a large number of devices such as fluorescent and incandescent lamps, refrigerators, heaters, compressors, motors, furnaces, and so on. The exact composition of load is difficult to estimate. Also, the composition varies significantly from region to region and changes depending on many factors including time (hour, day, season) and weather conditions. In power system stability and power flow studies, the common practice is to represent the composite load characteristics as seen from bulk power delivery points.

3.4.1 Static load models

A static load model expresses the characteristics of the load at any instant of time as algebraic functions of the bus voltage magnitude and frequency at that instant. The active power component P and the reactive power component Q are considered separately.

The characteristic of load changing with voltage is called the load voltage characteristic and the characteristic of load changing with frequency is called the load frequency characteristic.

Voltage dependency of load characteristics has been represented by the exponential model:

$$P_L = P_{L0}(\frac{V}{V_0})^{pv}(\frac{\omega}{\omega_0})^{p\omega} \tag{3.20}$$

$$Q_L = Q_{L0}(\frac{V}{V_0})^{qv}(\frac{\omega}{\omega_0})^{q\omega} \tag{3.21}$$

where P_0, Q_0, V_0, and ω_0 are power load, reactive power load, load bus voltage magnitude, and angle frequency, respectively.

A second model for representing load is the static load model, which is often expressed in polynomial form as below [14]:

$$P_L = P_{L0}[a_p(\frac{V}{V_0})^2 + B_p(\frac{V}{V_0}) + c_p](1 + p_\omega \Delta f) \tag{3.22}$$

$$Q_L = Q_{L0}[a_q(\frac{V}{V_0})^2 + B_q(\frac{V}{V_0}) + c_q](1 + q_\omega \Delta f) \tag{3.23}$$

If we neglect the load frequency sensitive part and only consider the load voltage sensitive part, Equations (3.22) and (3.23) can be simplified as:

$$P_L = P_{L0}[a_p(\frac{V}{V_0})^2 + B_p(\frac{V}{V_0}) + c_p] \tag{3.24}$$

$$Q_L = Q_{L0}[a_q(\frac{V}{V_0})^2 + B_q(\frac{V}{V_0}) + c_q] \tag{3.25}$$

The static load voltage sensitive model characterized in equations (3.24) and (3.25) is used in this research.

In power system analysis, we sometimes take all load in the system as constant impedance load, which is also called a linear load model. The kind of model can speed up calculations, but it represents a simplification that can result in significant error.

3.4.2 Load models and small signal stability damping studies

In small signal stability damping studies, inter-area modes of oscillation, involving a number of generators widely distributed over the power system, often result in significant variations in voltage and local frequency. The load voltage and frequency characteristics may have a significant effect on the damping of the oscillations. Using a constant impedance load representation in small signal analysis tends to overestimate the damping by 25 % compared with a more accurate load representation [22].

3.5 Overall system model

The power system stability problem can be represented by two sets of equations, which are, a set of differential equations to describe the dynamics of the synchronous generators and control devices and a set of algebraic equations to describe the transmission systems' response.

The differential set of the equations is dominated by the state space equations of the generators and controllers as shown in sections 3.2 and 3.3. These equations are (3.2), (3.3), (3.3) and (3.19).

The algebraic set of the equations is dominated by the network equations (power flow equations). The choice of equations and variables describing the network is normally one of the following:

- Real and imaginary parts of complex voltage are used as variables. The balance equations are real and imaginary part of injected current.

- Voltage magnitude and phase angle are used as variables. The balance equations are active and reactive power.

The latter alternative is used in this research work. Thus, the network equations to be satisfied are:

$$\Delta P_i = P_{Ei} - P_{Li} - V_i \sum_{k=1}^{n} V_k (G_{ik} \cos\theta_{ik} + B_{ik} \sin\theta_{ik}) = 0 \tag{3.26}$$

$$\Delta Q_i = Q_{Ei} - Q_{Li} - V_i \sum_{k=1}^{n} V_k (G_{ik} \sin\theta_{ik} - B_{ik} \cos\theta_{ik}) = 0 \tag{3.27}$$

$$(i = 1, 2, ..., n)$$

where P_{Ei} and Q_{Ei} are expressed in equations (3.8) and (3.9), while P_{Li} and Q_{Li} are expressed in equations (3.24) and (3.25).

Thus, the equations to describe the oscillatory behavior of a power system is a mix of differential and algebraic equations and can be expressed as:

$$\dot{x_1} = f(x_1, x_2) \tag{3.28}$$

$$0 = g(x_1, x_2) \tag{3.29}$$

where x_2 denotes voltage magnitude and phase angle, and x_1 denotes state variables of the system, which are:

- The angular positions and the angular velocities of the rotors of the machines
- The electro-magnetic state variables of machines
- The state variables relating to the excitation control systems
- The state variables relating to the speed-governor systems

After linearization, we get:

$$\begin{bmatrix} \Delta\dot{x_1} \\ 0 \end{bmatrix} = \begin{bmatrix} A_{11} & A_{12} \\ A_{21} & A_{22} \end{bmatrix} \begin{bmatrix} \Delta x_1 \\ \Delta x_2 \end{bmatrix} \tag{3.30}$$

where Δx_1 and Δx_2 denote small perturbations around an operating point. And

$$\begin{aligned} A_{11} &= \frac{\partial f}{\partial x_1}|_{x_{10},x_{20}} \\ A_{12} &= \frac{\partial f}{\partial x_2}|_{x_{10},x_{20}} \\ A_{21} &= \frac{\partial g}{\partial x_1}|_{x_{10},x_{20}} \\ A_{22} &= \frac{\partial g}{\partial x_2}|_{x_{10},x_{20}} \end{aligned}$$

The formulation of the state equations for small-signal analysis involves the development of linearized equations about an operating point and elimination of all variables other than the state variables. Thus, the formulation of the system matrix is:

$$\Delta \dot{x_1} = A_s \Delta x_1 \tag{3.31}$$

where

$$A_s = A_{11} - A_{12} A_{22}^{-1} A_{21} \tag{3.32}$$

After we get the system matrix A_s, we can use small signal stability method which we have discussed in Chapter 2 to analyze the system stability and to perform sensitivity analysis.

4 SENSITIVITY ANALYSIS OF TRANSMISSION SYSTEM

In this chapter, eigenvalue sensitivity to a parameter (line susceptance) is developed in section 4.1 (method 1), and functional sensitivity to $X_{TCSC}(s)$ is developed in section 4.2 (method 2). Both of the methods can be used to identify effective TCSC locations. A comparison is made between use of the system matrix A_s (method 1A and 2A) and original matrix A (method 1B, 1C and 2B) in both methods.

4.1 Eigenvalue sensitivity to line susceptance: method 1

We desire to compute the sensitivity of eigenvalues to a parameter p of the state matrix. The traditional approach to calculating eigenvalue sensitivity, see e.g.[23], requires the formulation of the system matrix A_s, which lacks sparsity. In another approach [24], a sensitivity formula is derived from a sparse formulation of the power system equations that works directly with the original A matrix. Below is a detailed description of these two methods as applied in computing eigenvalue sensitivity to line susceptance.

4.1.1 Using system matrix A_s: method 1A

4.1.1.1 General method description

The conventional method is based on the formulation of the system matrix A_s (recall from Equation (3.31), $\Delta\dot{x} = A_s\ \Delta x$). The expression of sensitivity of an eigenvalue λ_i

with respect to a certain parameter, p, can be written as,

$$\frac{\partial \lambda_i}{\partial p} = \frac{\psi_i \frac{\partial A_s}{\partial p} \phi_i}{\psi_i \phi_i} \tag{4.1}$$

where ψ_i and ϕ_i are the left and right eigenvectors of A_s (see section 2.3.1 for derivation).

4.1.1.2 Eigenvalue sensitivity to line susceptance

The expression for eigenvalue sensitivity with respect to line susceptance B_l is:

$$\frac{\partial \lambda_i}{\partial B_l} = \frac{\psi_i \frac{\partial A_s}{\partial B_l} \phi_i}{\psi_i \phi_i} \tag{4.2}$$

As shown in equation (3.32)

$$A_s = A_{11} - A_{12} A_{22}^{-1} A_{21} \tag{4.3}$$

so

$$\begin{aligned} \frac{\partial A_s}{\partial B_l} = \frac{\partial A_{11}}{\partial B_l} &- \frac{\partial A_{12}}{\partial B_l} A_{22}^{-1} A_{21} \\ &- A_{12} \frac{\partial A_{22}^{-1}}{\partial B_l} A_{21} \\ &- A_{12} A_{22}^{-1} \frac{\partial A_{21}}{\partial B_l} \end{aligned} \tag{4.4}$$

In equation (4.4) the part $\partial A_{22}^{-1} / \partial B_l$ is derived as follows:

Since

$$A_{22}^{-1} A_{22} = I \tag{4.5}$$

We may take the partial derivative of the above equation to obtain

$$\frac{\partial A_{22}^{-1}}{\partial B_l} A_{22} + A_{22}^{-1} \frac{A_{22}}{\partial B_l} = 0$$

Then:

$$\frac{\partial A_{22}^{-1}}{\partial B_l} = -A_{22}^{-1} \frac{\partial A_{22}}{\partial B_l} A_{22}^{-1} \tag{4.6}$$

Because the state variables (speeds, angles, etc.) and bus voltages (magnitude and phase angle) are dependent on line parameter B_l, we need to apply the chain rule of partial differentiation to every part of expression in (4.4). For example:

$$\frac{\partial A_{11}}{\partial B_l} = \frac{\partial A_{11}}{\partial B_l}|_{V,\theta} + \frac{\partial A_{11}}{\partial V}|_{B_l,\theta}\frac{\partial V}{\partial B_l} + \frac{\partial A_{11}}{\partial \theta}|_{B_l,V}\frac{\partial \theta}{\partial B_l} \tag{4.7}$$

where $\frac{\partial V}{\partial B_l}$ and $\frac{\partial \theta}{\partial B_l}$ are regarded as indirect sensitivity; and the terms with $\frac{\partial V}{\partial B_l}$ and $\frac{\partial \theta}{\partial B_l}$ are regarded as indirect sensitivity components.

As one can see from equations (4.2) to (4.7), there are significant drawbacks of the conventional method:

- The biggest drawback of this method is that we need to calculate the inverse of a matrix A_{22}^{-1} which has the same size as the Jacobian matrix in power flow. The matrix can be as large as 10,000 × 10,000.
- Matrix A_{22} itself is a sparse matrix, but the inverse of it is not. So we can not use sparse techniques while calculating the sensitivity.

4.1.2 Using the original matrix A: method 1B

4.1.2.1 General method description

Due to the drawbacks of the sensitivity analysis by using system matrix formulation, a new method for sensitivity analysis by using the original matrix A is presented in [24]. This new method is derived for a sparse formulation. It has been used in sensitivity analysis of power modulation, generators, static var compensators, HVDC system constraints, etc [24], but it has not been applied to computing sensitivity to line susceptance. The analysis is based on the formulation of the problem as a general differential-algebraic problem:

$$B\dot{x} = Ax \tag{4.8}$$

where B is a diagonal matrix with entry '1' for differential equations and entry '0' for algebraic equations.

Let ϕ_i and ψ_i denote the right and left eigenvectors corresponding to the generalized eigenvalue problem. The eigenvectors can be chosen so that the following conditions are satisfied for each eigenvalue.

$$A\phi_i = \lambda_i B\phi_i \tag{4.9}$$

$$\psi_i A = \lambda_i \psi_i B \tag{4.10}$$

$$\psi_i B\phi_i = 1 \tag{4.11}$$

Differentiating (4.9) with respect to a parameter p gives

$$\frac{\partial A}{\partial p}\phi_i + A\frac{\partial \phi_i}{\partial p} = \frac{\partial \lambda_i}{\partial p}B\phi_i + \lambda_i\frac{\partial B}{\partial p}\phi_i + \lambda_i B\frac{\partial \phi_i}{\partial p} \tag{4.12}$$

Premultiplying (4.12) by ψ_i gives

$$\psi_i\frac{\partial A}{\partial p}\phi_i + \psi_i A\frac{\partial \phi_i}{\partial p} = \frac{\partial \lambda_i}{\partial p}\psi_i B\phi_i + \psi_i\lambda_i\frac{\partial B}{\partial p}\phi_i + \lambda_i\psi_i B\frac{\partial \phi_i}{\partial p} \tag{4.13}$$

$$\psi_i\frac{\partial A}{\partial p}\phi_i = \frac{\partial \lambda_i}{\partial p}\psi_i B\phi_i + \lambda_i\psi_i B\frac{\partial \phi_i}{\partial p} \tag{4.14}$$

So, the sensitivity formula with respect to a parameter p can be given as [24]:

$$\frac{\partial \lambda_i}{\partial p} = \frac{\psi_i\frac{\partial A}{\partial p}\phi_i - \lambda_i\psi_i\frac{\partial B}{\partial p}\phi_i}{\psi_i B\phi_i} \tag{4.15}$$

For our problem, $B = \begin{bmatrix} I & 0 \\ 0 & 0 \end{bmatrix}$ because the bottom equations in equation (4.8) are algebraic (see equation (3.30)). Therefore, $\frac{\partial B}{\partial p} = 0$. Thus,

$$\frac{\partial \lambda_i}{\partial p} = \frac{\psi_i\frac{\partial A}{\partial p}\phi_i}{\psi_i B\phi_i} \tag{4.16}$$

4.1.2.2 Some comments

Although equation (4.16) is easy to derive and looks a lot like equation (4.1), there is a significant difference. Both A and B in equation (4.15) are sparse, and the parameters with respect to which we want to study the eigenvalue sensitivity typically affect only a few elements in A or B. Equally important, there is no need to calculate A_{22}^{-1}. But what is the relationship between the method of equation (4.1) and the method of equation (4.16)?

Suppose we have triple λ, ϕ, ψ which satisfy equations (4.9) and (4.10), the relationships can also be written as (4.17) and (4.18) if we let $\psi_i = \begin{bmatrix} \psi_{i1} & \psi_{i2} \end{bmatrix}$, and $\phi_i = \begin{bmatrix} \phi_{i1} \\ \phi_{i2} \end{bmatrix}$.

$$\begin{bmatrix} A_{11} & A_{12} \\ A_{21} & A_{22} \end{bmatrix} \begin{bmatrix} \phi_{i1} \\ \phi_{i2} \end{bmatrix} = \begin{bmatrix} \lambda_i \phi_{i1} \\ 0 \end{bmatrix} \tag{4.17}$$

$$\begin{bmatrix} \psi_{i1} & \psi_{i2} \end{bmatrix} \begin{bmatrix} A_{11} & A_{12} \\ A_{21} & A_{22} \end{bmatrix} = \begin{bmatrix} \lambda_i \psi_{i1} & 0 \end{bmatrix} \tag{4.18}$$

Eliminating ϕ_{i2} and ψ_{i2}, using $A_s = A_{11} - A_{12}A_{22}^{-1}A_{21}$, we obtain:

$$A_s \phi_{i1} = \lambda_i \phi_{i1} \tag{4.19}$$

$$\psi_{i1} A_s = \psi_{i1} \lambda_i \tag{4.20}$$

Comparing equation (4.17) with (4.19), and equation (4.18) with (4.20), we note that:

- For any triple $\lambda_i, \phi_{i1}, \phi_{i2}$ that satisfies (4.17) the pair λ_i, ϕ_{i1} satisfies (4.19). Conversely, if λ_i, ϕ_{i1} satisfies (4.19), then $\lambda_i, \phi_{i1}, \phi_{i2}$ satisfies (4.17), if $\phi_{i2} = -A_{22}^{-1}A_{21}\phi_{i1}$.

- For any triple $\lambda_i, \psi_{i1}, \psi_{i2}$ that satisfies (4.18) the pair λ_i, ψ_{i1} satisfies (4.20). Conversely, if λ_i, ψ_{i1} satisfies (4.20), then $\lambda_i, \psi_{i1}, \psi_{i2}$ satisfies (4.18), if $\psi_{i2} = -\psi_{i1}A_{12}A_{22}^{-1}$.

It may be easier to understand the problem if we look at it in the following way:

$$\begin{aligned}
\psi_{i1}\frac{\partial A_s}{\partial p}\phi_{i1} &= \psi_{i1}\left[\frac{\partial A_{11}}{\partial p} - \frac{\partial A_{12}}{\partial p}A_{22}^{-1}A_{21} + A_{12}A_{22}^{-1}\frac{\partial A_{21}}{\partial p}\right]\phi_{i1} \\
&= \begin{bmatrix}\psi_{i1} & -\psi_{i1}A_{12}A_{22}^{-1}\end{bmatrix}\begin{bmatrix}\frac{\partial A_{11}}{\partial p} & \frac{\partial A_{12}}{\partial p} \\ \frac{\partial A_{21}}{\partial p} & \frac{\partial A_{22}}{\partial p}\end{bmatrix}\begin{bmatrix}\phi_{i1} \\ -A_{22}^{-1}A_{21}\phi_{i1}\end{bmatrix} \qquad (4.21) \\
&= \begin{bmatrix}\psi_{i1} & \psi_{i2}\end{bmatrix}\begin{bmatrix}\frac{\partial A_{11}}{\partial p} & \frac{\partial A_{12}}{\partial p} \\ \frac{\partial A_{21}}{\partial p} & \frac{\partial A_{22}}{\partial p}\end{bmatrix}\begin{bmatrix}\phi_{i1} \\ \phi_{i2}\end{bmatrix} \\
&= \psi_i\left[\frac{\partial A}{\partial p}\right]\phi_i
\end{aligned}$$

4.1.2.3 Eigenvalue Sensitivity to line susceptance

As we know from Chapter 3, the power system stability problem can be represented by two sets of equations, which are, a set of differential equations to describe the dynamics of the synchronous generators and a set of algebraic equations to describe the transmission systems' response. So it is a differential-algebraic problem as described by equation (3.30) in chapter 3, repeated here for convenience:

$$A = \begin{bmatrix}A_{11} & A_{12} \\ A_{21} & A_{22}\end{bmatrix}$$

We may rewrite this as:

$$B_s\begin{bmatrix}\Delta\dot{x}_1 \\ \Delta\dot{x}_2\end{bmatrix} = A\begin{bmatrix}\Delta x_1 \\ \Delta x_2\end{bmatrix} \qquad (4.22)$$

where $A = \begin{bmatrix}A_{11} & A_{12} \\ A_{21} & A_{22}\end{bmatrix}$ and B_s is a diagonal matrix with entry '1' for differential equations and entry '0' for algebraic equations. Also, x_1 denotes state variables and x_2 denotes voltage angle and magnitude. As we can see, equation (4.22) has the same form as equation (4.8).

Both A and B in equation (4.15) are sparse, and a change in line susceptance affects much fewer elements in the A matrix than in A_s. Also we have:

$$\frac{\partial B_s}{\partial B_l} = 0 \tag{4.23}$$

so the sensitivity with regard to line susceptance is:

$$\frac{\partial \lambda_i}{\partial B_l} = \frac{\psi_i \frac{\partial A}{\partial B_l}\phi_i - \lambda_i \psi_i \frac{\partial B_s}{\partial B_l}\phi_i}{\psi_i B_s \phi_i} \tag{4.24}$$

and with $\frac{\partial B_s}{\partial B_l} = 0$,

$$\frac{\partial \lambda_i}{\partial B_l} = \frac{\psi_i \frac{\partial A}{\partial B_l}\phi_i}{\psi_i B_s \phi_i} \tag{4.25}$$

We see from equation (4.25) that we may obtain $\frac{\partial \lambda_i}{\partial B_l}$ if we can compute $\frac{\partial A}{\partial B_l}$. To this end, we note that, state variables, voltage magnitudes and phase angles are all dependent on the line parameter B_l, i.e.,

$$\begin{aligned} x_1 &= h_1(B_l) \\ x_2 &= h_2(B_l) \end{aligned} \tag{4.26}$$

Therefore, by the chain rule for partial differentiation,

$$\frac{\partial A}{\partial B_l} = \left[\begin{matrix} \frac{\partial A_{11}}{\partial B_l} & \frac{\partial A_{12}}{\partial B_l} \\ \frac{\partial A_{21}}{\partial B_l} & \frac{\partial A_{22}}{\partial B_l} \end{matrix}\right]\Bigg|_{x_{10},x_{20}} + \left[\begin{matrix} \frac{\partial A_{11}}{\partial x_1} & \frac{\partial A_{12}}{\partial x_1} \\ \frac{\partial A_{21}}{\partial x_1} & \frac{\partial A_{22}}{\partial x_1} \end{matrix}\right]\Bigg|_{B_l,x_{20}} \frac{\partial x_1}{\partial B_l} + \left[\begin{matrix} \frac{\partial A_{11}}{\partial x_2} & \frac{\partial A_{12}}{\partial x_2} \\ \frac{\partial A_{21}}{\partial x_2} & \frac{\partial A_{22}}{\partial x_2} \end{matrix}\right]\Bigg|_{B_l,x_{10}} \frac{\partial x_2}{\partial B_l} \tag{4.27}$$

The partial derivatives $\partial x_1/\partial B_l$ and $\partial x_2/\partial B_l$ in (4.27) are obtained at the equilibrium point of the system, i.e., for a given operating condition.

4.1.2.4 Calculation of $\partial x_1/\partial B_l$ and $\partial x_2/\partial B_l$

The equilibrium point of the system can be expressed from equations (3.28) and (3.29) as:

$$\begin{aligned} 0 &= f(x_1, x_2, B_l) \\ 0 &= g(x_1, x_2, B_l) \end{aligned} \tag{4.28}$$

Taking the partial derivative with respect to B_l for both equations, we obtain:

$$\frac{\partial f}{\partial B_l} = A_{11}\frac{\partial x_1}{\partial B_l} + A_{12}\frac{\partial x_2}{\partial B_l} \tag{4.29}$$

$$\frac{\partial g}{\partial B_l} = A_{21}\frac{\partial x_1}{\partial B_l} + A_{22}\frac{\partial x_2}{\partial B_l} \tag{4.30}$$

so that:

$$\begin{bmatrix} \frac{\partial x_1}{\partial B_l} \\ \frac{\partial x_2}{\partial B_l} \end{bmatrix} = \begin{bmatrix} A_{11} & A_{12} \\ A_{21} & A_{22} \end{bmatrix}^{-1} \begin{bmatrix} \frac{\partial f}{\partial B_l} \\ \frac{\partial g}{\partial B_l} \end{bmatrix} \tag{4.31}$$

We can use Gauss Elimination to get the left-hand side of equation (4.31).

As one can see from the above, method 1A and method 1B involve complicated differential calculations. Method 1B avoids the calculation of inverse of matrix A_{22}. Matrix A retains its sparsity while matrix A_s does not. Also, a sparse technique can be used to calculate the eigenvalues and eigenvectors of matrix A. In the thesis, method 1B is used to calculate the eigenvalue sensitivity with respect to line susceptance.

4.1.2.5 Flow chart to carry out parameter sensitivity analysis to B_l

Calculation for method 1B are carried out as shown in Fig. 4.1.

4.1.2.6 An approximation of method 1B: method 1C

For a long time, calculations have been done for eigenvalue sensitivity to a parameter such as K_A and T_A of exciters, and etc. without considering the indirect sensitivity components which were based on the assumption that the influence of the indirect sensitivity

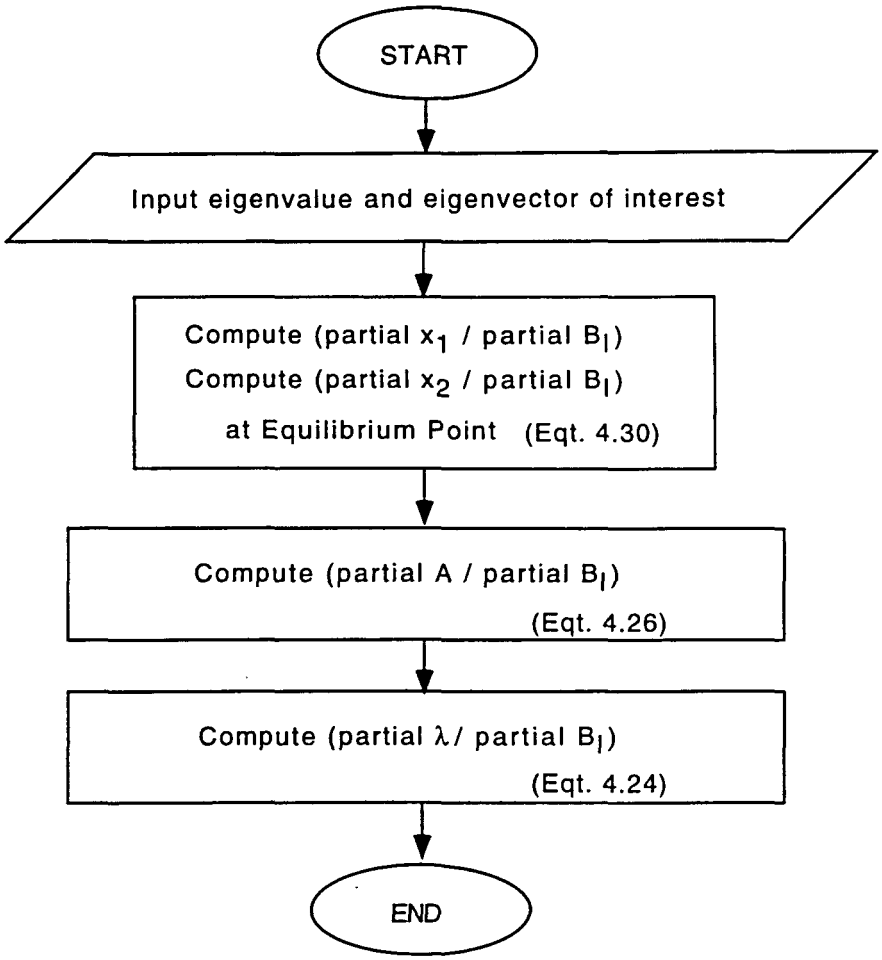

Figure 4.1 Flow chart for method 1B

components are not large enough to be influential. In this section, an approximation is made to the method 1B in order to test this assumption for sensitivity to B_l.

Equation (4.27) indicates that $\frac{\partial A}{\partial B_l}$ is comprised of three terms.

- Variation in A matrix elements directly caused by variation in B_l
- Variation in A matrix elements indirectly caused by variation in B_l through variation in x_1
- Variation in A matrix elements indirectly caused by variation in B_l through variation in x_2

Of these, the influence of the first term is expected to be significant whereas the influence of term 2 and 3 may not be, i.e. $\partial x_1/\partial B_l \approx 0$ and $\partial x_2/\partial B_l \approx 0$. If so, the eigenvalue sensitivity to line susceptance will be:

$$\frac{\partial \lambda_i}{\partial B_l} = \frac{\psi_i \frac{\partial A}{\partial B_l} \phi_i}{\psi_i \phi_i} \tag{4.32}$$

where

$$\frac{\partial A}{\partial B_l} = \left[\begin{array}{cc} \frac{\partial A_{11}}{\partial B_l} & \frac{\partial A_{12}}{\partial B_l} \\ \frac{\partial A_{21}}{\partial B_l} & \frac{\partial A_{22}}{\partial B_l} \end{array} \right]_{x_{10}, x_{20}} \tag{4.33}$$

Calculation of $\frac{\partial \lambda_i}{\partial B_l}$ using equation (4.33) instead of equation (4.27) regarded as the approximate method 1C in Chapter 5.

In Chapter 5, two examples are given to compare the different results between methods with and without this approximation. The examples show that we cannot ignore the indirect sensitivity components.

4.2 Functional sensitivity to $X_{TCSC}(s)$: method 2

4.2.1 Functional sensitivity to $X_{TCSC}(s)$ using system matrix: method 2A

Let the overall system be represented by:

$$\Delta \dot{X} = A_s \Delta X + b \Delta u \tag{4.34}$$

$$\Delta y = c \Delta X \tag{4.35}$$

where the input signal used in this study is the transmission line susceptance, and output signal is the speed difference between two areas. Let

$$\Delta u = X_{TCSC}(s)\, \Delta y \tag{4.36}$$

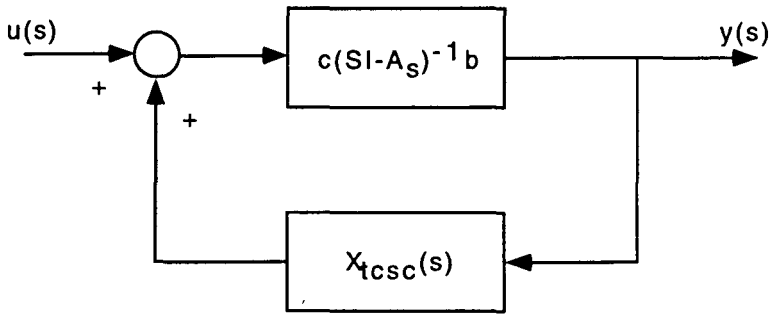

Figure 4.2 System transfer function with TCSC

Then

$$\Delta\dot{X} = (A_s + b\ X_{TCSC}\ c)\Delta X \tag{4.37}$$

Now let

$$A_c = A_s + b\ X_{TCSC}\ c \tag{4.38}$$

Then we have:

$$(\lambda_i I - A_c)\phi_i = 0 \tag{4.39}$$

$$\psi_i(\lambda_i I - A_c) = 0 \tag{4.40}$$

where ϕ_i and ψ_i are the right and left eigenvector, respectively, of A_c.

Differentiating (4.40), we get:

$$(\frac{\partial\lambda_i}{\partial X_{TCSC}}I - \frac{\partial A_c}{\partial X_{TCSC}})\phi_i + (\lambda_i\ I - A_c)\frac{\partial\phi_i}{\partial X_{TCSC}} = 0 \tag{4.41}$$

Premultiplying by ψ_i,

$$\psi_i(\frac{\partial\lambda_i}{\partial X_{TCSC}}I - \frac{\partial A_c}{\partial X_{TCSC}})\phi_i + \psi_i(\lambda_i\ I - A_c)\frac{\partial\phi_i}{\partial X_{TCSC}} = 0 \tag{4.42}$$

By equation (4.40), the second term in equation (4.42) is zero and

$$\psi_i(\frac{\partial\lambda_i}{\partial X_{TCSC}}I - \frac{\partial A_c}{\partial X_{TCSC}})\phi_i = 0 \tag{4.43}$$

Manipulating equation (4.43), we obtain

$$\frac{\partial \lambda_i}{\partial X_{TCSC}} = \frac{\psi_i \dfrac{\partial A_c}{\partial X_{TCSC}} \phi_i}{\psi_i \phi_i} \tag{4.44}$$

Since $A_c = A_s + b\ X_{TCSC}(\lambda_i)\ c$,

$$\frac{\partial A_c}{\partial X_{TCSC}(\lambda_i)} = b\ c \tag{4.45}$$

Therefore equation (4.44) becomes

$$\frac{\partial \lambda_i}{\partial X_{TCSC}(\lambda_i)} = \psi_i\ b\ c\ \phi_i \tag{4.46}$$

which is defined as the functional sensitivity of λ_i to $X_{TCSC}(s)$.

4.2.1.1 Calculation of A_s and b

We presented in the previous section how to get the functional sensitivity to $X_{TCSC}(s)$. In this section, we derive the form of matrices A_s and b. The original nonlinear system is:

$$\dot{x}_1 = f(x_1, x_2, u) \tag{4.47}$$

$$0 = g(x_1, x_2, u) \tag{4.48}$$

After linearization of the above equations, we get:

$$\Delta\dot{x}_1 = \frac{\partial f}{\partial x_1}\Delta x_1 + \frac{\partial f}{\partial x_2}\Delta x_2 + \frac{\partial f}{\partial u}\Delta u \tag{4.49}$$

$$0 = \frac{\partial g}{\partial x_1}\Delta x_1 + \frac{\partial g}{\partial x_2}\Delta x_2 + \frac{\partial g}{\partial u}\Delta u \tag{4.50}$$

From the above equations, we get:

$$\Delta x_2 = \frac{\partial g}{\partial x_2}^{-1}\left[\frac{\partial g}{\partial x_1}\Delta x_1 + \frac{\partial g}{\partial u}\Delta u\right] \tag{4.51}$$

and finally,

$$\begin{aligned} \Delta\dot{x}_1 &= \left[\frac{\partial f}{\partial x_1} - \frac{\partial f}{\partial x_2}\frac{\partial g}{\partial x_2}^{-1}\frac{\partial g}{\partial x_1}\right]\Delta x_1 \\ &+ \left[\frac{\partial f}{\partial u} - \frac{\partial f}{\partial x_2}\frac{\partial g}{\partial u}^{-1}\frac{\partial g}{\partial u}\right]\Delta u \end{aligned} \tag{4.52}$$

so:

$$\begin{aligned} A_s &= \frac{\partial f}{\partial x_1} - \frac{\partial f}{\partial x_2}\frac{\partial g}{\partial x_2}^{-1}\frac{\partial g}{\partial x_1} \\ b &= \frac{\partial f}{\partial u} - \frac{\partial f}{\partial x_2}\frac{\partial g}{\partial x_2}^{-1}\frac{\partial g}{\partial u} \end{aligned} \tag{4.53}$$

4.2.1.2 Input signal of TCSC and c matrix

According to different control law of TCSC, we can use different signals and therefore have different c matrices. For example in this study, for a TCSC in transmission line l with input signal $\Delta\omega_i - \Delta\omega_j$, we have:

$$c = [0, 0, 0, ..., \underset{i}{1}, ..., \underset{j}{-1}, ...0] \tag{4.54}$$

4.2.2 Functional sensitivity to $X_{TCSC}(s)$ using original matrix: method 2B

As discussed in section 4.1.2.3 and 4.2.1.1, the overall system can be represented as:

$$\begin{aligned} B_s \begin{bmatrix} \Delta\dot{x}_1 \\ \Delta\dot{x}_2 \end{bmatrix} &= A \begin{bmatrix} \Delta x_1 \\ \Delta x_2 \end{bmatrix} + b_1\ \Delta u \\ y &= c_1 \begin{bmatrix} \Delta x_1 \\ \Delta x_2 \end{bmatrix} \end{aligned} \tag{4.55}$$

where $b_1 = \begin{bmatrix} \partial f/\partial u \\ \partial g/\partial u \end{bmatrix}$, and $c_1 = \begin{bmatrix} c & \mathbf{0} \end{bmatrix}$. c here is the same as in equations (4.37).

Since

$$u = X_{TCSC}\, y \tag{4.56}$$

and with

$$\Delta X = \begin{bmatrix} \Delta x_1 \\ \Delta x_2 \end{bmatrix}$$

Then,

$$\Delta \dot{X} = (A + b_1\, X_{TCSC}\, c_1)\Delta X \tag{4.57}$$

Now let,

$$A_c = A + b_1\, X_{TCSC}\, c_1 \tag{4.58}$$

Following the steps in section 4.1.2.1, we can get:

$$\frac{\partial \lambda_i}{\partial X_{TCSC}} = \frac{\psi_i \frac{\partial A}{\partial X_{TCSC}} \phi_i - \lambda_i \psi_i \frac{\partial B_s}{\partial X_{TCSC}} \phi_i}{\psi_i B_s \phi_i} \tag{4.59}$$

since

$$\frac{\partial B_s}{\partial X_{TCSC}} = 0 \tag{4.60}$$

and $A_c = A + b_1\, X_{TCSC}\, c_1$,

$$\frac{\partial A_c}{\partial X_{TCSC}} = b_1\, c_1 \tag{4.61}$$

The functional sensitivity to $X_{TCSC}(s)$ is:

$$\frac{\partial \lambda_i}{\partial X_{TCSC}} = \psi_i\, b\, c\, \phi_i \tag{4.62}$$

Although the form of the functional sensitivity in equation (4.62) is exactly the same as the one using system matrix, several major difference should be noticed:

- The left and right eigenvector in (4.62) are generalized eigenvectors.

- Let the system have n state variables and m algebraic variables. For the method using system matrix (A_s), the column vector b is a $n \times 1$ matrix, row vector c is a $1 \times n$ matrix; while for the method that uses the original matrix (A), the column vector b is $(n+m) \times 1$, and row vector c is a $1 \times (n+m)$ matrix.
- The column vector b in (4.62) is just $[\partial f/\partial u, \partial g/\partial u]^T$.
- Need not to calculate the inverse of matrix A_{22} as the elimination of x_2 is not needed This is the most significant advantage by using original matrix A.
- With regard to computation time, using original matrix is much faster.

4.2.2.1 Flow chart to carry out functional sensitivity analysis to $X_{TCSC}(s)$

Calculation for method 2B are carried out as shown in Fig. 4.3.

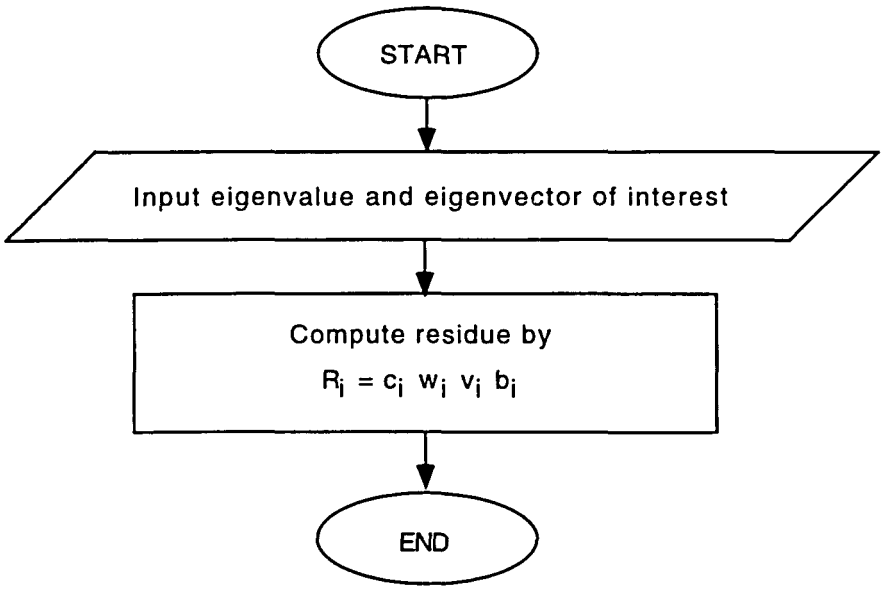

Figure 4.3 Flow chart for method 2B

4.3 Discussion

Functional sensitivity provides us with the effect on λ_i of controlling line susceptance, whereas parameter sensitivity provides us with the effect on λ_i of changing line susceptance. Thus we have:

- For good damping effect from transient control point of view, use functional sensitivity.
- For good damping effect from steady state control, use parameter sensitivity.

If the criteria for the best location for TCSC is having best damping effect from transient and steady state control, then both the parameter sensitivity and functional sensitivity should be used to make the choice.

However, it seems intuitively that if one line has the greatest effect on λ_i of changing susceptance of line, it should have the greatest effect on λ_i of controlling susceptance of line. So, what is the relationship between functional sensitivity and parameter sensitivity, i.e., what is the relationship between effect on λ_i of controlling susceptance of line and changing susceptance of line? This question is under investigation.

5 EIGENVALUE SENSITIVITY ANALYSIS TEST SYSTEM

The results of eigenvalue sensitivity to line susceptance and the results of functional sensitivity of $X_{TCSC}(s)$ can be used to determine the location of TCSC. This chapter contains numerical results on different issues discussed in Chapter 4. The results are presented on the following:

- Two examples are given to show the importance of including indirect sensitivity $\frac{\partial x_1}{\partial B_l}$ and $\frac{\partial x_2}{\partial B_l}$.
- Examples are given to illustrate and compare the method of eigenvalue sensitivity to line susceptance (method 1) and the method of functional sensitivity to $X_{TCSC}(s)$ (method 2).
- The influence of operating conditions are investigated.

5.1 The need to include indirect sensitivity components

As indicated before, the only difference between method $1B$ and method $1C$ is method $1C$ does not take into account the changes in indirect sensitivity (voltage magnitude, phase angle and state variables) while there is a small change in line susceptance B_l (i.e., we approximate that $\Delta x_1 = 0$, $\Delta V = 0$ and $\Delta\theta = 0$). In this section, we will investigate how much it will affect the value and the ranking of the sensitivity list in a one machine to infinite bus system and a multi-machine system.

Table 5.1 Sensitivity result using method 1 and 2

sensitivity value	*method 1B*	*method 1C*
$\mid \frac{\partial \lambda}{\partial B_l} \mid$	j0.9697	j0.7273

5.1.1 Example one: one machine to infinite bus system

The objective of using one machine to infinite bus system as an example is to illustrate that neglecting of the change in x_1 (state variables) and x_2 (voltage magnitude and phase angle) with the change in B_l will lead to errors.

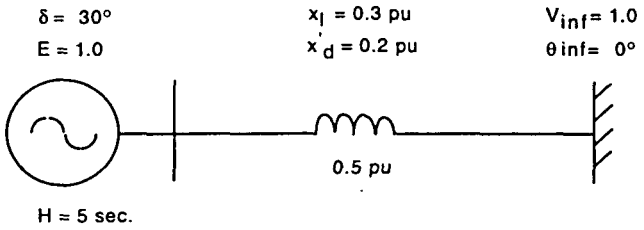

Figure 5.1 System structure of example 1

The system of Fig. 5.1 has one electro-mechanical mode with eigenvalues $\pm j8.0806$. Given a very small change in $B_l = 0.01$, recalculate the eigenvalues of the system to obtain $\pm j8.0903$. So, we have,

$$\mid \frac{\Delta \lambda}{\Delta B_l} \mid = \frac{j.009697}{0.01} = j0.9697$$

The sensitivity result using method $1B$ and method $1C$ is given in Table 5.1. This result indicates that the result from method $1B$ is correct, and neglecting the changes in x_1 and x_2 will cause approximately 25% error in a one machine to infinite bus system. In the next section, a multi-machine system is studied to show the importance to include the indirect sensitivity components.

5.1.2 Example 2: multi-machine system

5.1.2.1 System description

A 3-area, 6-machine power system is used to illustrate the method of using modal sensitivity analysis with respect to line susceptance to obtain the potential TCSC location. The system is shown in Fig. 5.2. The system has three areas. Machines 1 and 2 form the area C, machines 3 and 4 form the area B, and machines 5 and 6 form the area A. All system parameters are expressed on a 1000 MVA base. In this system, 814 MW of the power produced by machines 3 and 4 and 775 MW of the power produced by machines 5 and 6 is exported and consumed by the load L_1 and L_2.

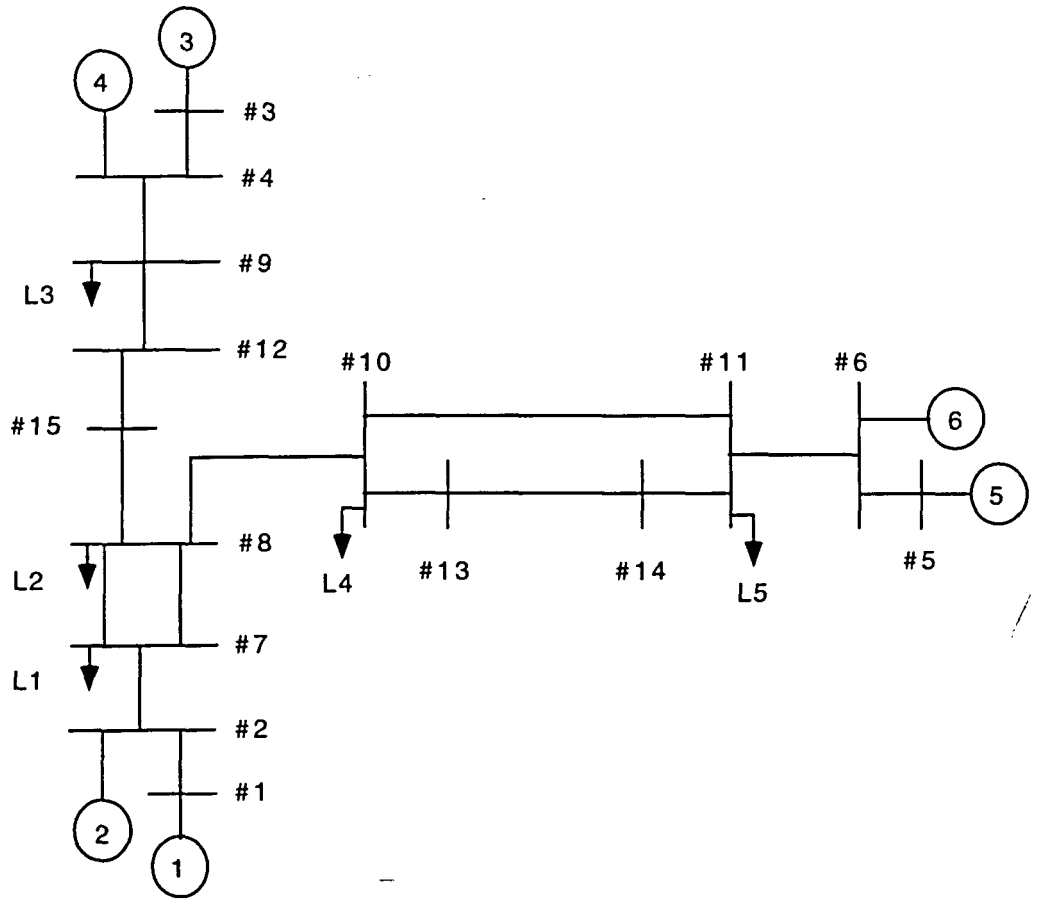

Figure 5.2 System structure of example 2

We use a third order model for all generators and a first order model for the exciters. Parameters, given on the machine base, are the same for the machines [11]. The system has five electro-mechanical modes. The eigenvalues of the system are given in Table 5.2. The first inter-area mode consists of machines of area A oscillating against those in area B and C (Mode 1), and the second inter-area mode consists of the machines of area B oscillating against the machines of area C (Mode 2). The other three modes are the local modes of machine oscillations within the areas. The system has one unstable mode (inter-area mode 1).

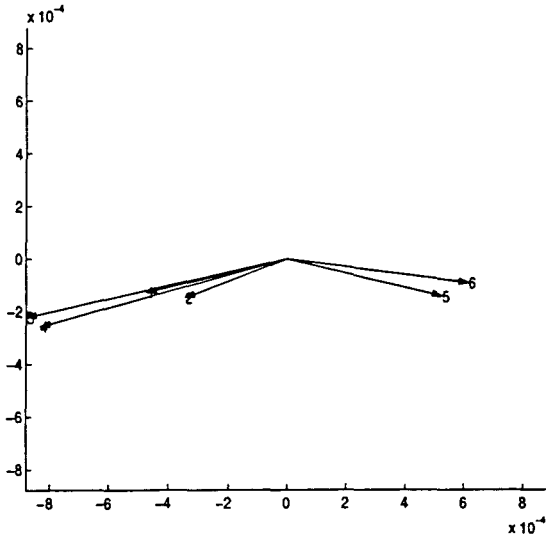

Figure 5.3 Modeshape of mode 1

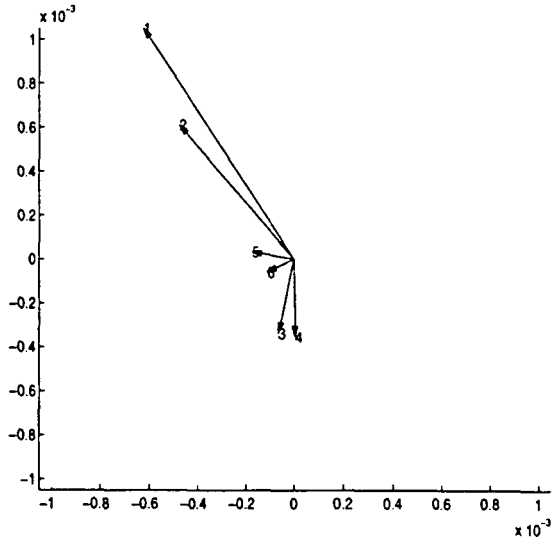

Figure 5.4 Modeshape of mode 2

The mode shapes of the two inter-area modes are shown in Fig. 5.3 and 5.4. The mode shape of the three plant modes are shown in Fig. 5.5 to Fig. 5.7. Whether a mode is plant or inter-area is determined by the modeshape. For the local modes, the units oscillate in almost anti-phase, and have almost the same amplitudes. For the inter-area modes, the phase difference between the generating units in the two areas is noticeably less than 180^o and they have different amplitude. We focus on sensitivity analysis on the inter-area modes.

Table 5.2 Eigenvalue of the system

No.	*eigenvalue*	*mode*
1	-86.593	
2	-90.846	
3	-88.998	
4	-98.582	
5	-98.452	
6	-98.390	
7	-14.120	
8	-1.7520	
9	-12.193	
10	-8.8147	
11	-0.50905+ 12.209i	plant mode
12	-0.50905- 12.209i	C
13	-0.62935+ 11.194i	plant mode
14	-0.62935- 11.194i	A
15	-0.64494+ 10.767i	plant mode
16	-0.64494- 10.767i	B
17	-0.54911+ 6.4194i	inter-area
18	-0.54911- 6.4194i	mode 2
19	0.078826+ 4.4680i	inter-area
20	0.078826- 4.4680i	mode 1
21	-0.71429	
22	-1.7277+ 0.026699i	
23	-1.7277- 0.026699i	

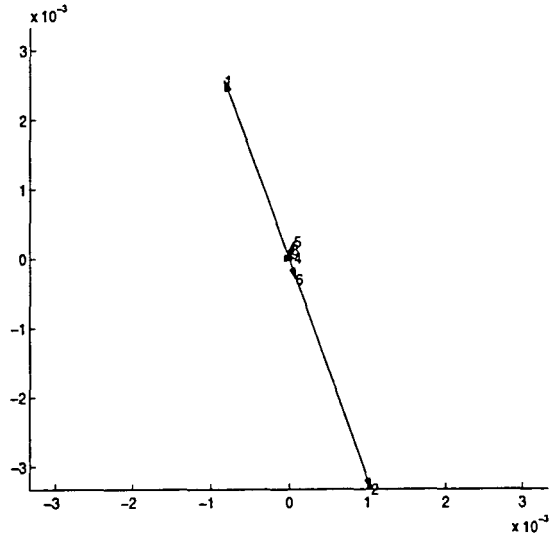

Figure 5.5 Modeshape of plant mode C

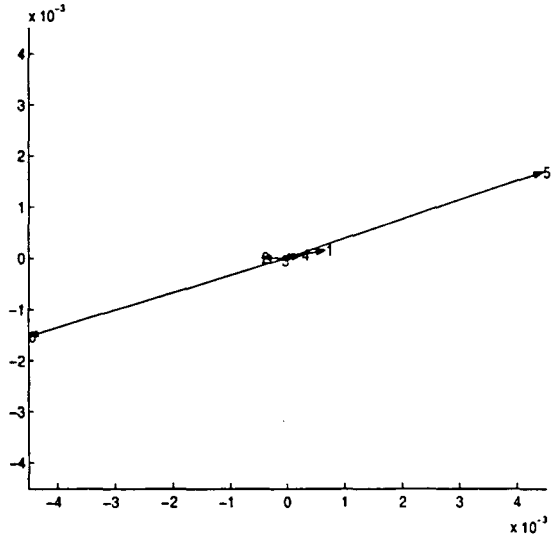

Figure 5.6 Modeshape of plant mode A

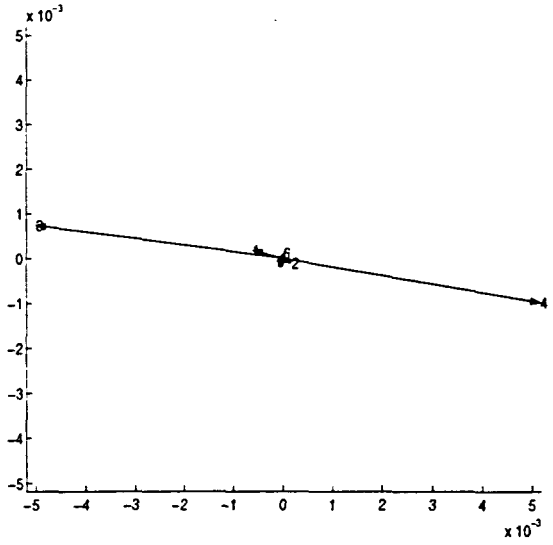

Figure 5.7 Modeshape of plant mode B

5.1.2.2 Comparison of sensitivity results of method $1B$ and $1C$

In the example, we use two methods (methods $1B$ and $1C$) to determine the best location of TCSC for damping mode 1. As explained in section 4.1.2, method $1B$ includes the indirect sensitivity components and method $1C$ does not.

Table 5.3 summarizes the most effective transmission lines for locating TCSC from greatest to least by using method $1B$ and method $1C$. As we can see from Table 5.3, the sensitivity values of the two methods are much different from each other; this also results in difference in ranking.

From the method $1B$ results of Table 5.3, we can determine that the line from bus 10 to 11 has the highest sensitivity value. As one can see from Fig. 5.2, the line between bus 10 to 11 is the corridor that connects area A to the rest of system. Also, from the figure 5.3, we know that the swing mode (mode 1) to be controlled is the mode for which the machines 5 and 6 swing against the rest of the machines in the system (machine 1,2, 3 and 4). Thus, the results in the table agree with intuition.

We may notice that the values of the highest ones differ most, and values of the lowest one differs least. This implies that the influence of indirect sensitivity components (voltage magnitude, phase angle and state variables) is greatest on eigenvalue sensitivity to line susceptance in the most sensitive transmission lines. Evidence for this is provided in Table 5.4 which gives the norm of the sensitivity of the indirect sensitivity to line susceptance for each of the lines in the system.

We conclude from examples 1 and 2 that the indirect sensitivity components are significant and their influence must be included when computing eigenvalue sensitivity to line susceptance.

Table 5.3 Comparison of method 1B and 1C for mode 1

rank	*method* 1*B*		*method* 1*C*	
	line No.	value[a]	line No.	value
1	10-11	2.0175	12-9	0.24946
2	13-14	1.2488	10-11	0.15735
3	12-9	0.47992	13-14	0.093904
4	11-6	0.19102	11-6	0.044607
5	8-10	0.095320	8-10	0.038207
6	7-8	0.061177	9-4	0.011097
7	2-7	0.033752	6-5	0.0089698
8	11-14	0.017863	7-8	0.0085102
9	10-13	0.017863	11-14	0.0051517
10	9-4	0.011161	10-13	0.0045786
11	6-5	0.0045819	4-3	0.0031222
12	4-3	0.0032495	2-7	0.0013104
13	1-2	0.0014472	1-2	0.00060595
14	12-15	0.00019197	8-15	0.00016416
15	8-15	0.00019197	12-15	0.00016114

[a]Unless indicated otherwise, the term "value" is regard as absolute value of sensitivity throughout this chapter.

Table 5.4 2-norm of $\frac{\partial X}{\partial B_l}$

rank	*line No.*	*2-norm* $\frac{\partial X}{\partial B_l}^a$
1	10-11	1.9953
2	13-14	1.2133
3	12-9	0.67274
4	11-6	0.19624
5	9-4	0.078099
6	2-7	0.076414
7	7-8	0.075847
8	8-10	0.075256
9	11-14	0.024728
10	6-5	0.024447
11	1-2	0.023052
12	10-13	0.022738
13	4-3	0.018574
14	8-15	0.00030938
15	12-15	0.00028993

$^aX = [x_1\ x_2]^T$,

$\| X \|_2 = (X, X)^{1/2} = (\sum_{i=1}^{n} x_i^2)^{1/2}$

5.2 Comparison of method $1B$ and method $2B$

In this section, a comparison is made between parameter sensitivity to line susceptance and functional sensitivity to transmission line controller TCSC. Method $1B$ uses parameter sensitivity to determine the TCSC effectiveness; in method $2B$ we use functional sensitivity for the same purpose. For the TCSC control channel, we use the speed difference between two areas as an input signal and the transmission line susceptance as an output signal in this study.

From Table 5.5, we can see that the line from bus 10 to bus 11 also has the highest functional sensitivity value (residue). Therefore both methods result in identification of the same line for TCSC effectiveness. The result of method $1B$ gives the change of eigenvalue when we introduce a small change in B_l from the system operating point of view; method $2B$ gives some information on the location of a certain control loop from the system dynamic performance point of view. Specifically, in this case it gives information when we close the control loop from speed difference to line susceptance. With the exception of line $9-4$, both methods rank the remaining lines in the same order. The influence on line $9-4$ sensitivity is the subject of ongoing investigation.

5.3 Influence of operating condition to sensitivity result

The inter-area modes and their damping values vary as system operating conditions (flows, load levels, etc.) change. In this section we investigate how change in operating condition influence our ranking list in TCSC effectiveness.

Table 5.5 Comparison of results of method $1B$ and $2B$

rank	*method* $1B$		*method* $2B$	
	line No.	value	line No.	value
1	10-11	2.0175	10-11	0.18888
2	13-14	1.2488	13-14	0.11668
3	12-9	0.19102	12-9	0.063657
4	11-6	0.47992	11-6	0.018758
5	8-10	0.095320	9-4	0.0088305
6	7-8	0.061177	8-10	0.0077386
7	2-7	0.033752	7-8	0.0047555
8	11-14	0.017863	2-7	0.0023593
9	10-13	0.017863	11-14	0.0017867
10	9-4	0.011161	10-13	0.0017867
11	6-5	0.0045819	6-5	0.0011144
12	4-3	0.0032495	4-3	0.00066688
13	1-2	0.0014472	1-2	0.00037306
14	12-15	0.00019197	12-15	0.000025463
15	8-15	0.00019197	8-15	0.000025463

Table 5.6 Eigenvalue with the variation in $Z_{9,12}$

mode	*stiff*	*medium*	*weak*
	0.2 pu	0.3 pu	0.5 pu
1	-0.057134 ± 5.4235i	-0.012774 ± 5.1877i	0.078826 ± 4.4680i
2	-0.48906 ± 7.6576i	-0.49884 ± 7.2458i	-0.54911± 6.4194i

Table 5.7 Parameter sensitivity result with change in $Z_{9,12}$

rank	*stiff (0.2 pu)*		*medium (0.3 pu)*		*weak (0.5 pu)*	
	line No.	value	line No.	value	line No.	value
1	10-11	1.3461	10-11	1.4486	10-11	2.0175
2	13-14	0.81742	13-14	0.88579	13-14	1.2488
3	11-6	0.12019	12-9	0.13649	12-9	0.19102

5.3.1 Operation condition varied by tie-line strength variations

The system operating condition can be stiff, medium or weak with variations in tie-line reactance $Z_{9,12}$. Table 5.6 gives the eigenvalues of mode 1 for changes in $Z_{9,12}$.

We investigated the ranking list of sensitivity analysis for damping mode 1. Table 5.7 shows the result of method $1B$ (parameter sensitivity) and Table 5.8 shows the result of method $2B$ (functional sensitivity). We note that the two methods are in agreement with respect to the ranking value obtained for each operating condition. We note also that under every operating condition, the line which has the largest sensitivity is always line $10-11$.

Table 5.7 and Table 5.8 also indicate that as the system becomes weaker, the sensitivity value becomes larger, i.e., the influence of a series capacitor to system stability depends on the line reactance and becomes larger when the line reactance increases.

Note that the ranking for the stiff condition of the system is different from the ranking for the other conditions. In the weak and medium conditions, the change in susceptance of line $12-9$ has a greater effect on the eigenvalue than does a change in line $11-6$ susceptance, but under the stiff condition, line $12-9$ has a lesser effect on the eigenvalues than does a change in line $11-6$ susceptance. The explaination of this is the subject of current investigation.

Table 5.8 Functional sensitivity result with change in $Z_{9,12}$

rank	*stiff (0.2 pu)*		*medium (0.3 pu)*		*weak (0.5 pu)*	
	line No.	value	line No.	value	line No.	value
1	10-11	0.10436	10-11	0.12800	10-11	0.18888
2	13-14	0.061796	13-14	0.076709	13-14	0.11668
3	11-6	0.0098800	12-9	0.017273	12-9	0.063657

Table 5.9 Eigenvalue with the variation in L_1 and G_3

mode	*light* ($\Delta L_1 = 0.0pu$)	*medium* ($\Delta L_1 = 0.1pu$)	*heavy* ($\Delta L_1 = 0.2pu$)
1	-.012774 ± 5.1877i	.017034 ± 5.0147i	.047594 ± 4.6414i
2	-.49884 ± 7.2458i	-.46320 ± 7.1638i	-.42623 ± 7.0137i

5.3.2 Operation condition varied by changing generation and load level

For the case when $Z_{9,12} = 0.3\ pu$, we consider operating conditions with load level change in L_1; this change is balanced by changing the generation level of generator No. 3 or generator No. 5. Both generators in areas A and B send power to area C. System loading conditions can be light, medium, and heavy depending on the change in the pair L_1 and G_3 representing power transfer between area B and C (scenario one), or the pair L_1 and G_5 representing power transfer between the area A and C (scenario two). Table 5.10 summarizes the results of scenario one; and Table 5.12 summarizes the results of

Table 5.10 Parameter sensitivity result with change in L_1 and G_3

rank	*light* ($\Delta L_1 = 0.0pu$)		*medium* ($\Delta L_1 = 0.1pu$)		*heavy* ($\Delta L_1 = 0.2pu$)	
	line No.	value	line No.	value	line No.	value
1	10-11	1.4486	10-11	1.7436	10-11	2.5256
2	13-14	0.88579	13-14	1.0725	13-14	1.5674
3	12-9	0.13649	11-6	0.16118	11-6	0.23989

Table 5.11 Eigenvalue with the variation in L_1 and G_5

mode	*light* ($\Delta L_1 = -0.1pu$)	*medium* ($\Delta L_1 = 0.0pu$)	*heavy* ($\Delta L_1 = 0.06pu$)
1	-0.093404 ± 5.5628i	-0.012774 ± 5.1877i	0.047155 ± 4.6071i
2	-0.49715 ± 7.3298i	-0.49884 ± 7.2458i	-0.49980 ± 7.1543i

Table 5.12 Parameter sensitivity result with change in L_1 and G_5

rank	*light* ($\Delta L_1 = -0.1pu$)		*medium* ($\Delta L_1 = 0.0pu$)		*heavy* ($\Delta L_1 = 0.06pu$)	
	line No.	value	line No.	value	line No.	value
1	10-11	0.90277	10-11	1.4486	10-11	2.6367
2	13-14	0.54283	13-14	0.88579	13-14	1.6297
3	12-9	0.14619	11-6	0.13649	11-6	0.24970

scenario two.

From the results, we observe the same phenomena as we saw when changing $Z_{9,12}$: as the operating condition becomes more stressed, the sensitivity values increase. The transmission line from $10-11$ is still the most sensitive line. For this system, changes in the operating condition do not significantly effect the ranking list of the sensitivity results. We conclude that the most effective TCSC controller location for damping mode 1 is line $10-11$.

All of the sensitivity results in this section are obtained via the parameter sensitivity method, and the results will be very similar to those obtained via functional sensitivity method.

6 CONCLUSIONS

The objective of this thesis is to develop a method for identifying the most effective circuit for locating a TCSC. In the thesis, both parameter sensitivity method and functional sensitivity methods are used to determine the potential TCSC location in order to dampen a certain modes. The conclusion of this study are:

- While computing parameter sensitivity, we can not ignore the influence of the indirect sensitivity components (voltage magnitude, phase angle, and state variables) while changing line susceptance B_l.
- Both parameter sensitivity and functional sensitivity can be used to determine the location of TCSC. However, the two different methods give different information:
  - Parameter sensitivity method gives the information of what is the effect on λ_i of changing the susceptance of line from steady state point of view.
  - Functional sensitivity method gives the information of what is the effect on λ_i of controlling the susceptance of line from dynamic point of view.
- Based on the system studied in this work, the circuit ranking order tends to be similar using the two methods, but some difference do arise. Explanations for these differences are being investigated.

APPENDIX DATAFILE

BUS DATA FORMAT

bus:

number, voltage(pu), angle(degree), p_gen(pu), q_gen(pu), p_load(pu), q_load(pu), bus_type

bus_type

- 1, swing bus - 2, generator bus (PV bus) - 3, load bus (PQ bus)

1 1.05 0.00 0.90 0.30 0.00 0.00 0 0 2; gen#1

2 1.05 0.00 0.90 0.20 0.00 0.00 0 0 2; gen#2

3 1.05 0.00 0.80 0.20 0.00 0.00 0 0 2; gen#3

4 1.05 0.00 0.90 0.30 0.00 0.00 0 0 2; gen#4

5 1.05 0.00 0.90 0.20 0.00 0.00 0 0 2; gen#5

6 1.05 0.00 0.80 0.20 0.00 0.00 0 0 1; gen#6 (swing bus)

7 1.00 0.00 0.00 0.00 3.00 1.00 0 0 3; load#1

8 1.00 0.00 0.00 0.00 0.30 0.00 0 0 3; load#2

9 1.00 0.00 0.00 0.00 0.80 0.20 0 0 3; load#3

10 1.00 0.00 0.00 0.00 0.50 0.00 0 0 3; load#4

11 1.00 0.00 0.00 0.00 0.40 0.10 0 0 3; load#5

12 1.00 0.00 0.00 0.00 0.00 0.00 0 0 3;

13 1.00 0.00 0.00 0.00 0.00 0.00 0 0 3;

14 1.00 0.00 0.00 0.00 0.00 0.00 0 0 3;

15 1.00 0.00 0.00 0.00 0.00 0.00 0 0 3;

LINE DATA FORMAT

line: from bus, to bus, resistance(pu), reactance(pu), line charging(pu), tap ratio

1 2 0.010 0.10 0.000 1. 0;

2 7 0.005 0.05 0.000 1. 0;

7 8 0.010 0.10 0.000 1. 0;

12 9 0.080 0.80 0.000 1. 0;

9 4 0.010 0.10 0.000 1. 0;

4 3 0.010 0.10 0.000 1. 0;

8 10 0.010 0.10 0.000 1. 0;

10 11 0.080 0.80 0.000 1. 0;

11 6 0.010 0.10 0.000 1. 0;

6 5 0.010 0.10 0.000 1. 0;

10 13 0.040 0.10 0.000 1. 0;

13 14 0.000 0.60 0.000 1. 0;

11 14 0.040 0.10 0.000 1. 0;

8 15 0.001 0.01 0.000 1. 0;

12 15 0.001 0.01 0.000 1. 0;

MACHINE DATA FORMAT

machine:

1. machine number
2. bus number
3. machine base mva
4. leakage reactance x_l(pu)
5. resistance r_a(pu)
6. d-axis sychronous reactance x_d(pu)
7. d-axis transient reactance $x_d^{'}$(pu)
8. d-axis subtransient reactance $x_d^{"}$(pu)
9. d-axis open-circuit time constant $T_{do}^{'}$(sec)
10. d-axis open-circuit subtransient time constant $T_{do}^{"}$(sec)
11. q-axis sychronous reactance x_q(pu)
12. q-axis transient reactance $x_q^{'}$(pu)
13. q-axis subtransient reactance $x_q^{"}$(pu)
14. q-axis open-circuit time constant $T_{qo}^{'}$(sec)
15. q-axis open circuit subtransient time constant $T_q o^{"}$(sec)
16. inertia constant H(sec)
17. damping coefficient d_o(pu)
18. dampling coefficient d_1(pu)
19. bus number
20. S(1.0) - saturation factor
21. S(1.2) - saturation factor

1 1 900 0.2 0.0 1.8 0.3 0.25 8.0 0.03 1.7 0.55 0.25 0.4 0.05 3.5 5 0 1 0 0;

2 2 900 0.2 0.0 1.8 0.3 0.25 8.0 0.03 1.7 0.55 0.25 0.4 0.05 3.5 5 0 2 0 0;

3 3 900 0.2 0.0 1.8 0.3 0.25 8.0 0.03 1.7 0.55 0.25 0.4 0.05 3.5 5 0 4 0 0;

4 4 900 0.2 0.0 1.8 0.3 0.25 8.0 0.03 1.7 0.55 0.25 0.4 0.05 3.5 5 0 5 0 0;

5 5 900 0.2 0.0 1.8 0.3 0.25 8.0 0.03 1.7 0.55 0.25 0.4 0.05 3.5 5 0 4 0 0;

6 6 900 0.2 0.0 1.8 0.3 0.25 8.0 0.03 1.7 0.55 0.25 0.4 0.05 3.5 5 0 4 0 0;

EXCITER DATA FORMAT

exciter: 1. exciter type - 3 for ST3

2. machine number

3. input filter time constant T_R

4. voltage regulator gain K_A

5. voltage regulator time constant T_A

6. voltage regulator time constant T_B

7. voltage regulator time constant T_C

8. maximum voltage regulator output V_{Rmax}

9. minimum voltage regulator output V_{Rmin}

10. maximum internal signal V_{Imax}

11. minimum internal signal V_{Imin}

12. first stage regulator gain K_J

13. potential circuit gain coefficient K_p

14. potential circuit phase angle θ_p

15. current circuit gain coefficient K_I

16. potential source reactance X_L

17. rectifier loading factor K_C

18. maximum field voltage E_{fdmax}

19. inner loop feedback constant K_G

20. maximum inner loop voltage feedback V_{Gmax}

0 1 0.0 100 0.01 10 1 5 -5;

0 2 0.0 100 0.01 10 1 5 -5;

0 3 0.0 100 0.01 10 1 5 -5;

0 4 0.0 100 0.01 10 1 5 -5;

0 5 0.0 100 0.01 10 1 5 -5;

0 6 0.0 100 0.01 10 1 5 -5;

BIBLIOGRAPHY

[1] Narain G. Hingorani, "FACTS flexible AC transmission system," *The Second Annual Transmission and Wheeling Conference*, November 1991.

[2] IEEE Power Engineering Society, "FACTS Applications," Tech. Rep. TP 116-0, IEEE, 1996.

[3] IEEE Power Engineering Society, "FACTS Overview," Tech. Rep. TP 108, IEEE and CIGRE, 1995.

[4] Narain G. Hingorani, "The energy policy act compels utilities to unbundle generation, transmission, and distribution," *IEEE Spectrum*, pp. 60–61, January 1994.

[5] P. M. Anderson and A. A. Fouad, *Power System Control and Stabiltiy.* IEEE Press, New York, 1994.

[6] P. M. Anderson and R. G. Farmer, *Series Compensation of Power System.* PBLSH! Inc., Encinitas, California, 1996.

[7] Sasan G. Jalali, Ron A. Hedin, Macros Pereira and Kadry Sadek, "A stability model for the advanced series compensator (ASC)," *IEEE Transactions on Power Delivery*, vol. 11, pp. 1128–1137, April 1996.

[8] Narain G. Hingorani, "FACTS flexible AC transmission system," *IEE Fifth International Conference on AC and DC Power Transmission*, September 1991.

[9] S.G.Helbing and G.G.Karady, "Investigations of an advanced form of series compensation," *IEEE Transactions on Power Delivery*, vol. 9, pp. 939–947, April 1994.

[10] E. Larsen, C. Bowler, B. Damsky, and S. Nilsson, "Benefits of thyristor controlled series compensation." CIGRE 1992 joint section 14/37/38, Paris, August, 1992.

[11] J. H. Chow, "Concepts for design of facts controllers to damp power swings," *IEEE Transactions on Power Systems*, vol. 10, pp. 948–956, May 1995.

[12] M. Noroozian and G. Andersson, "Damping of inter-area and local modes by use of controllable components," *IEEE Transactions on Power Delivery*, vol. 10, pp. 2007–2012, October 1995.

[13] F. deMello, "Exploratory concepts on control of variable series compensation in transmission systems to improve damping of intermachine oscillations." IEEE-PES Winter Meeting, 1993, Paper 93 WM 208.

[14] P. Kundur, *Power System Stability and Control.* McGraw-Hill Inc., New York, 1993.

[15] E. F. V. Arcidiacono and R. Marconato, "Evaluation and improvement of electromechanical oscillation damping by means of eigenvalue-eigenvector analysis," *IEEE Transaction on Power Apparatus and Systems*, vol. PAS-99, pp. 769–777, March/April 1980.

[16] F. Luis Pagola, Ignacio J. Perez-Arriaga and George C. Verghese, "On sensitivities, residues and participations: Applications to oscillatory stabiltiy analysis and control," *IEEE Transaction on Power Systems*, vol. 4, pp. 278–285, Februray 1989.

[17] E. Zhou, "Functional sensitivity concept and its application to power system," *IEEE Transactions on Power Systems*, vol. 9, pp. 518–524, February 1994.

[18] X. Yang and A. Feliachi, "Stabilization of inter-area oscillation modes through excitation systems," *IEEE Transactions on Power Systems*, vol. 9, pp. 494–500, Feb. 1994.

[19] X. R. Chen, "Design of TCSC controllers to damp power swings by using eigenvalue analysis method." IEEE / KTH Conference, June, 1995.

[20] N. Martins, "Oscillation damping analysis and control studies of the future interconnection between the north-northeast and south-southeast systems." V Symposium of Specialists in Electric Operational and Expansion Planning, May, 1996.

[21] Xiaoxin Zhou, Hanxiang Li and Zhongxi Wu, *Power System Analysis*. EPRI Press, Beijing, China, 1989.

[22] IEEE Task Force on Load Representation for Dynamic Performance, "Load representation for dynamic performance analysis," *IEEE Transactions on Power Systems*, vol. 8, pp. 472–482, May 1993.

[23] N. S. P. Nolan and R. Alden, "Eigenvalue sensitivities of power systems including network and shate dynamics," *IEEE Trans. Power App. and Sys.*, vol. PAS-95, pp. 1318–1324, 1976.

[24] T. Smed, "Feasible eigenvalue sensitivity for large power systems," *IEEE Trans. on Power Systems*, vol. 8, pp. 555–561, May 1993.